AFWAL-TR-80-4001

ADA087846

AN EXPERIMENTAL WEIGHT FUNCTION METHOD FOR STRESS INTENSITY FACTOR CALIBRATION

Dan Bar-Tikva, Major, IAF

Metals Behavior Branch
Metals and Ceramics Division

DTIC
S ELECTE D
AUG 1 3 1980
B

April 1980

TECHNICAL REPORT AFWAL-TR-80-4001

Interim Report for Period January 1979 - October 1979

DDC FILE COPY

80 8 13 088

NOTICE

When Government drawings, specifications, or other data are used for any pur-
pose other than in connection with a definitely related Government procurement
operation, the United States Government thereby incurs no responsibility nor any
obligation whatsoever; and the fact that the Government may have formulated,
furnished, or in any way supplied the said drawings, specifications, or other
data, is not to be regarded by implication or otherwise as in any manner licen-
sing the holder or any other person or corporation, or conveying any rights or
permission to manufacture, use, or sell any patented invention that may in any
way be related thereto.

This report has been reviewed by the Information Office (OI) and is releasable
to the National Technical Information Service (NTIS). At NTIS, it will be avail-
able to the general public, including foreign nations.

This technical report has been reviewed and is approved for publication.

DR. T. NICHOLAS
Metals Behavior Branch
Metals and Ceramics Division

NATHAN G. TUPPER, Chief
Metals Behavior Branch
Metals and Ceramics Division

"If your address has changed, if you wish to be removed from our mailing list,
or if the addressee is no longer employed by your organization please notify
AFWAL/MLLN, W-PAFB, OH 45433 to help us maintain a current mailing list".

Copies of this report should not be returned unless return is required by se-
curity considerations, contractual obligations, or notice on a specific document.

REPORT DOCUMENTATION PAGE	READ INSTRUCTIONS BEFORE COMPLETING FORM

1. REPORT NUMBER	2. GOVT ACCESSION NO.	3. RECIPIENT'S CATALOG NUMBER
AFWAL-TR-80-4001	AD-A087 846	

4. TITLE (and Subtitle)	5. TYPE OF REPORT & PERIOD COVERED
AN EXPERIMENTAL WEIGHT FUNCTION METHOD FOR STRESS INTENSITY FACTOR CALIBRATION	Interim Report, for period Jan 79 - Oct 79
	6. PERFORMING ORG. REPORT NUMBER

7. AUTHOR(s)	8. CONTRACT OR GRANT NUMBER(s)
Dan Bar-Tikva Major, IAF	

9. PERFORMING ORGANIZATION NAME AND ADDRESS	10. PROGRAM ELEMENT, PROJECT, TASK AREA & WORK UNIT NUMBERS
Materials Laboratory AF Wright Aeronautical Laboratories (AFSC) Wright-Patterson Air Force Base, Ohio 45433	2307 P1 02

11. CONTROLLING OFFICE NAME AND ADDRESS	12. REPORT DATE
Materials Laboratory AF Wright Aeronautical Laboratories (AFSC) Wright-Patterson Air Force Base, Ohio 45433	Apr 1980
	13. NUMBER OF PAGES
	93

14. MONITORING AGENCY NAME & ADDRESS(if different from Controlling Office)	15. SECURITY CLASS. (of this report)
	Unclassified
	15a. DECLASSIFICATION DOWNGRADING SCHEDULE

16. DISTRIBUTION STATEMENT (of this Report)

Approved for public release; distribution unlimited.

17. DISTRIBUTION STATEMENT (of the abstract entered in Block 20, if different from Report)

18. SUPPLEMENTARY NOTES

19. KEY WORDS (Continue on reverse side if necessary and identify by block number)

Stress Intensity Factor
Weight Function
Crack Opening
Fracture Mechanics

20. ABSTRACT (Continue on reverse side if necessary and identify by block number)

The weight function procedure allows one to convert stress intensity factors K and crack displacement information obtained for one crack configuration and loading into the stress intensity factor solution for the same geometry and another loading.

The feasibility of using the weight function idea for a two dimensional case with experimental results is demonstrated in this work. Mode I stress intensity factor K_1 measurements obtained by a laser interferometric technique and

DD FORM 1473 EDITION OF 1 NOV 65 IS OBSOLETE
1 JAN 73

392662

"crack mouth" opening displacement measurements were taken for an edge cracked strip subjected to four point bending. These results were used to construct (numerically) a weight function with the aid of a computer program written for this purpose.

Results of K_1 for the same geometry with two different loading configurations, uniform tension and three point bending (with two different length to width ratios) were computed.

These results agree favorably with the known solutions and demonstrate that a set of experiments for a single loading can accurately predict the stress intensity factor for any other loading configuration of the same geometry. The advantage of the weight function method would be particularly important if these loading configurations are difficult or impossible to reproduce in the laboratory.

AFWAL-TR-80-4001

FOREWORD

The work reported herein was conducted in the Metals Behavior Branch,
Metals and Ceramics Division, Materials Laboratory, Air Force Wright
Aeronautical Laboratories, Wright-Patterson Air Force Base, Ohio. The
research was conducted by Major Dan Bar-Tikva, IAF, in partial fulfill-
ment of the requirements for the degree of Master of Science, School
of Engineering of the Air Force Institute of Technology.

The author would like to express his gratitude to his thesis
advisors, Dr. A. F. Grandt of AFWAL (MLLN) and to Professor A. Palazotto,
AFIT Department of Aeronautics and Astronautics, for their guidance and
suggestions during the course of this investigation. The author would
also like to thank Dr. T. Nicholas of AFWAL (MLLN) for making available
the Mechanical Test Facility of the AFWAL (MLLN) Metals and Ceramics Division
and the engineering and technical staff of Systems Research Laboratories,
Dayton, Ohio for their invaluable assistance and advice.

The research was conducted during the period January 1979 to
October 1979. This report was submitted for publication in December 1979.

ACCESSION for

NTIS	White Section ✔
DDC	Buff Section ☐
UNANNOUNCED	☐
JUSTIFICATION	

BY
DISTRIBUTION/AVAILABILITY CODES

Dist.   AVAIL. and/or SPECIAL

A

AFWAL-TR-80-4001

TABLE OF CONTENTS

TABLE OF CONTENTS (CONCLUDED)

LIST OF ILLUSTRATIONS

LIST OF TABLES

LIST OF SYMBOLS

A	Area
a	Crack length
B	Coefficient defined by Equation
b	Material thickness
C	Compliance
c	Half the height of the beam W/2
d	Distance between indentation
E	Young elastic modulus
f	Body forces
G	Shear modulus
g	Griffith energy release rate

$$H \quad \begin{cases} E & \text{plane stress} \\ \dfrac{E}{1-\nu^2} & \text{plane strain} \end{cases}$$

h	Weight function
i,j,n	Indices
K	Stress intensity factor
$\overline{K}$	Curvature
K_I	Mode I stress intensity factor
$\overline{K}_I$	Nondimensional mode I stress intensity factor
K_{II}	Mode II stress intensity factor
K_{III}	Mode III stress intensity factor
K_{IC}	Mode I fracture toughness
k	Stress intensity factor per unit load
ℓ	Half span between supports
M	Moment
m	Fringe order
$\overline{m}$	Orange conic section coefficient

p	Crack surface tractions
P	Load
R	Coefficient defined by Equation (2-24)
$\bar{R}$	Radius of curvature
r	Radius from crack tip
r_p	Plastic zone radius
S	Span between supports
s	Path
T	Surface tractions
t	Coordinate along crack, starting at the crack tip
U	Total strain energy stored in the cracked body
u_i^m	Displacement at location i for load P_m
u_x	Displacement in x direction
u_y	Displacement in y direction
W	Beam or strip height
x,y	Cartesian coordinate
Y	Nondimensional stress intensity factor
α_o	Diffraction angle
Γ	Path
δd	Change in distance between indentations
δm	Change in fringe order
ϵ	Strain
η	Crack surface vertical displacement
η_o	Crack mouth vertical displacement
λ	Wave length
θ	Angular coordinate
ν	Poisson ratio
σ_{ij}	Stress components
σ_{ys}	Yield stress

SECTION I

INTRODUCTION

1. BACKGROUND

Fracture mechanics presently provides the best available tools to quantitatively assess the influence of preexistent cracks in structures. Although fracture mechanics, as we now know it, is a relatively new technology (since the mid 1950s), the basic ideas were already presented by Griffith (Reference 1) in the early 1920s.

Current linear elastic fracture mechanics (LEFM) concepts assume that the stress intensity factor K, the parameter that relates load, crack length, and geometry, controls fracture ($K = K_c$ = constant at fracture) and crack propagation (Reference 23).

Stress intensity factor calibrations are required for any fracture or crack propagation analysis. Since crack tip analysis can be complex, experimental K solutions often become necessary to verify or supplement analytical or numerical solutions.

For complex type geometries and loading configurations which commonly exist in aircraft structures, experimentation may be the primary method to obtain a reasonably accurate and dependable solution. Conducting experiments on actual parts and loadings is often a very difficult and costly procedure.

The main motivation for this investigation was to find a technique that may, in some cases, greatly reduce the experimental effort required in order to obtain a K solution.

An analytical approach to determine the stress intensity factors K was discussed by Bueckner (Reference 2) and Rice (Reference 3). They showed that once the displacement field and stress intensity factors are known for one geometry and loading configuration referred to subsequently as Case 1, K may be obtained for any other loading (Case 2) applied to the same crack geometry (References 4 through 8, 21). The method depends mainly on the reciprocal theorem and strain energy expressions. A load

and material independent weight function can be constructed to relate the stress intensity factor, material properties, and crack length together with crack surface opening (for more details see Part II and Appendix A).

The significant advantage of this procedure lies in the fact that only the first problem (Case 1) needs to be solved directly. Construction of the weight function for this case allows ready determination of K for any other loading on the same crack geometry (Cases 2, 3, etc.). Stress intensity factors may then be obtained for a variety of other specimen loadings, some of which may be highly complex compared to the original. In addition, the computational expenses are minimal because only a single relatively simple load configuration needs to be calculated.

The only additional information required for any other case is the stress distribution at the crack location for a noncracked body under the load configuration in question. This stress distribution is available, in many cases, from the static crack free stress analysis or can be obtained with much less effort than a cracked body analysis requires.

2. PURPOSE

Although weight functions have been employed with analytical, finite elements and other numerical methods, the author is unaware of attempts to combine weight functions with experimental procedures.

The objective of this work was to show that the weight function idea can assist the experimentalist by allowing him an opportunity to obtain the stress intensity factor solution for a complex loading configuration from the results of a simple experiment, and also to obtain K solutions for a variety of loadings from a single set of experiments. This will greatly reduce the complexity and scope of the experimental effort.

3. GENERAL APPROACH

The weight function procedure is demonstrated with experimental results for an edge crack specimen.

The reference (Case 1) problem has been chosen as an edge cracked strip subjected to four-point bending. Crack surface displacement measurements near the crack tip were obtained by a laser interferometric method following the technique developed at the Materials Laboratory (References 9, 10, 19). These results gave the mode I stress intensity factor K_I for that case. Crack mouth opening measurements, using a clip gage, were then used to construct the crack surface displacement function incorporating Orange (Reference 11) conic section approximation. These experimental results were used to evaluate the weight function and predict the stress intensity factor K_I for other cases, which were chosen to be uniform tension and three-point bending. The results were compared with the known solution given in References 12 through 14.

SECTION II

THEORY

1. GENERAL ASSUMPTIONS

    a. Linear elastic fracture mechanics (LEFM) applies i.e., the amount of plasticity near the crack tip is relatively small

$$\frac{r_p}{a} \leq 0.1$$

where r_p is the radius of plastic zone. (See Hertzberg, Reference 15, and Appendix B for a more detailed discussion.)

    b. The problem is assumed to be purely two-dimensional; i.e., no variations through the thickness are considered.

    c. Body forces are assumed to be negligible.

    d. Only pure Mode I crack openings will be discussed.

2. STRESS INTENSITY FACTOR

The stress intensity factor K is the LEFM parameter that relates load, crack length and geometry. The LEFM approach to predicting crack growth assumes that K controls:

    a. Fracture ($K = K_c$ = constant at fracture)

    b. Crack propagation due to fatigue

    c. Crack propagation due to stress corrosion

Three modes of stress intensity factors are defined depending on the crack tip opening mode (Figure 1). They may be stated as:

$$\text{Mode I} \quad \text{Opening } K_I = \lim_{r \to 0} \sqrt{2\pi r} \; \sigma_y \quad (\Theta = 0) \quad (1)$$

$$\text{Mode II} \quad \text{Sliding } K_{II} = \lim_{r \to 0} \sqrt{2\pi r} \; \sigma_{xy} \quad (\Theta = 0) \quad (2)$$

$$\text{Mode III} \quad \text{Tearing } K_{III} = \lim_{r \to 0} \sqrt{2\pi r} \; \sigma_{yz} \quad (\Theta = 0) \quad (3)$$

where crack tip coordinates are defined in Figure 2.
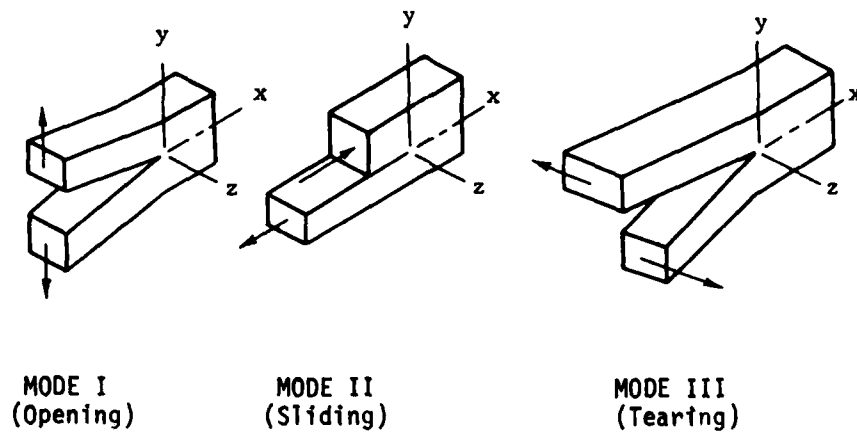
Figure 1.   Crack Opening Modes
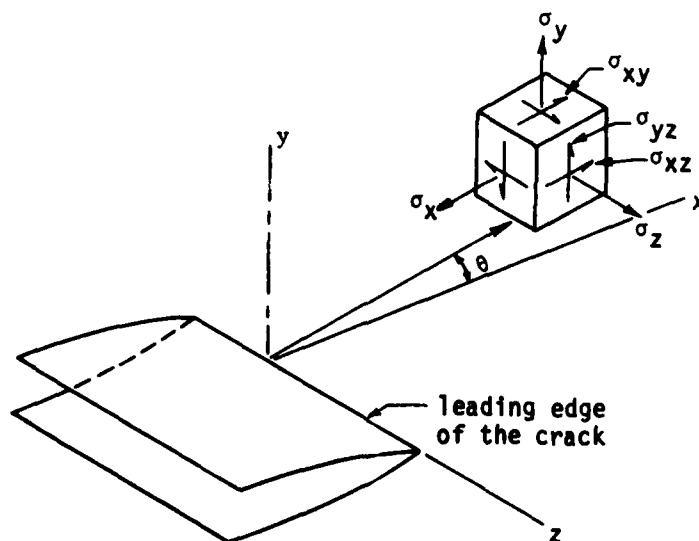
Figure 2.   Crack Tip Stress Coordinates

This work deals only with the opening Mode I, though it can be easily extended to other "modes."

3. THE WEIGHT FUNCTION

The Mode I stress intensity factor K_I under arbitrary loading, shown in Figure 3, can be given as:

$$K_I = \int_\Gamma T \cdot h \, d\Gamma + \int_A f \cdot h \cdot dA \qquad (4)$$

(see Appendix A and References 2 through 6 for detailed discussion).

where:

Γ is any path chosen around the body that includes all the surface tractions and body forces,

A is the region defined by Γ,

T designates surface tractions,

K_I is the Mode I stress intensity solution corresponding to the loads T and f,

f are body forces,

$h = h(x,y,a) = \dfrac{H}{2K_I} \dfrac{\partial \eta(x,y,a)}{\partial a}$ (the weight function) $\qquad (5)$

$\eta(x,y,a)$ is the crack vertical displacement for any chosen load configuration (independent of T and f),

K_I in the weight function, Equation 5, is the Mode I stress intensity solution that corresponds to the η solution, and

$$H = \begin{cases} E & \text{for plane stress} \\ \dfrac{E}{1-\nu^2} & \text{for plane strain.} \end{cases}$$

The weight function h is independent of the loads T, f, and material properties and can be calculated for the same geometry from another known solution of K_I and $\partial \eta / \partial a$.
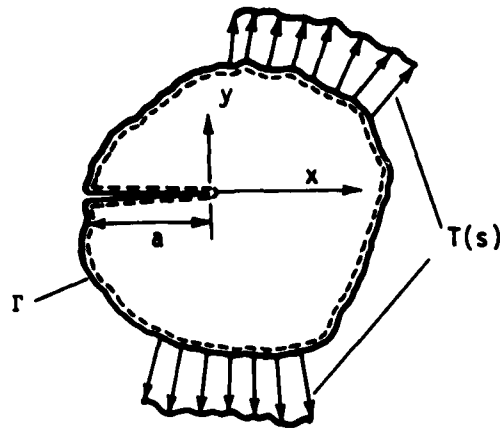
Figure 3. Cracked Body Loading Configuration

Using the principle of superposition of linear elasticity, the calculations of the stress intensity factor considering the case of a cracked body under a certain loading configuration is equal to the case of the cracked body where only the crack surface is subjected to tractions $p(x)$ (coordinates are chosen so that the crack is in x direction). Here $p(x)$ is the stress σ_y that will occur at the crack location for an uncracked body subjected to the original loading configuration. This idea is demonstrated in Figure 4.

If one chooses the path Γ as any path that includes the crack surface and, for simplicity, takes a straight crack in the x-direction as in Figure 4 (the last assumption is not essential and is used only to simplify the equations), then Equation 4 for K_I can be stated as:

$$K_I = \int_0^a h(x,a)\,p(x)\,dx - \int_a^0 h(x,a)\,p(x)\,dx \qquad (6)$$

Reversing the integration limits and adding the two integrals we get:

$$K_I = 2\int_0^a h(x,a)\,p(x)\,dx \qquad (7)$$

7
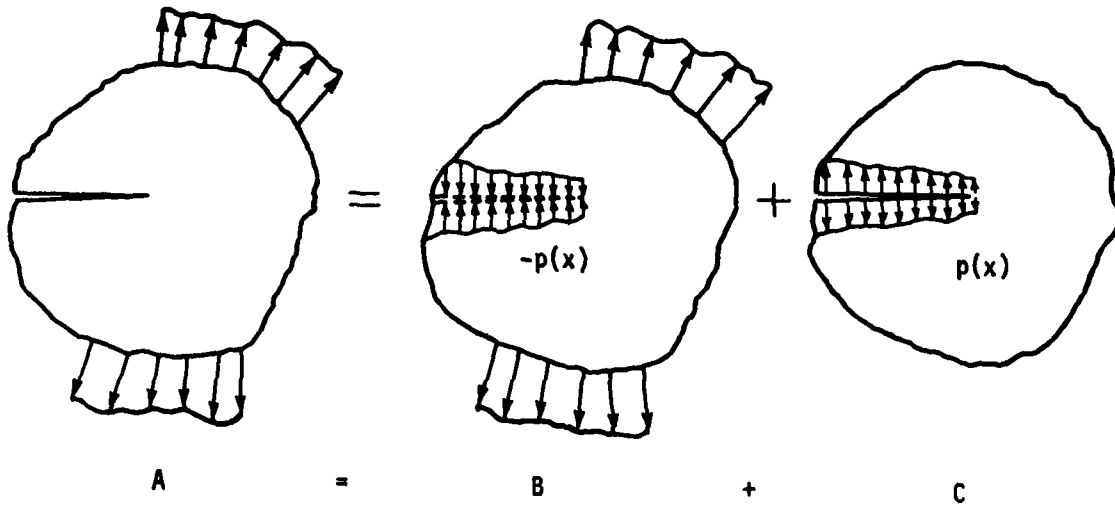
Figure 4. Superposition

$$K_{I_{\textcircled{A}}} = K_{I_{\textcircled{B}}} + K_{I_{\textcircled{C}}}$$

Part B can be viewed as a noncracked body; therefore,

$$K_{I_{\textcircled{B}}} = 0 \implies K_{I_{\textcircled{A}}} = K_{I_{\textcircled{C}}}$$

The unknown stress intensity solution for the loading $p(x)$ is considered Case 2, and the known solution, from which the weight function will be computed, is taken as Case 1. Then Equation 7 can be written as

$$K_{I_{\textcircled{2}}} = 2 \int_{0}^{a} h_{\textcircled{1}}(x,a) \, p_{\textcircled{2}}(x) \, dx \tag{8}$$

and from Equation 5

$$h_{\textcircled{1}}(x,a) = \frac{H}{2 K_{I_{\textcircled{1}}}} \left(\frac{\partial \eta(x,a)}{\partial a} \right)_{\textcircled{1}} \tag{9}$$

8

If Equation 9 is substituted into Equation 8, the result is:

$$K_{I_{②}} = \frac{H}{K_{I_{①}}} \int_0^a p(x)_{②} \left(\frac{\partial \eta(x,a)}{a} \right)_{①} dx \qquad (10)$$

where

$K_{I_{②}}$ is the Mode I stress intensity factor to be found,

$p(x)_{②}$ is the stress σ_y at the crack location for a noncracked body with loading configuration of Case 2,

$K_{I_{①}}$ is the Mode I stress intensity factor for Case 1 and will be determined experimentally, and

$\frac{\partial \eta}{\partial a}_{①}$ is the derivative with respect to crack length of the crack opening profile for Case 1. η is also determined experimentally.

4. K CALIBRATION BY CRACK TIP DISPLACEMENT

The crack tip displacement field is defined by the following relations that represent the elasticity solution for the stress-displacement field in terms of K near the crack tip of a cracked body. One can take these displacement expressions for Mode I opening (References 17, 18, 10) as:

$$u_x = \frac{K_I}{G} \sqrt{\frac{r}{2\pi}} \cos \frac{\theta}{2} \left[\frac{1-\nu}{1+\nu} + \sin^2 \frac{\theta}{2} \right] \qquad (11)$$

$$u_y = \frac{K_I}{G} \sqrt{\frac{r}{2\pi}} \sin \frac{\theta}{2} \left[\frac{2}{1+\nu} - \cos^2 \frac{\theta}{2} \right] \qquad (12)$$

for plane stress; and

$$u_x = \frac{K_I}{G} \sqrt{\frac{r}{2\pi}} \cos \frac{\Theta}{2} \left[1-2\nu + \sin^2 \frac{\Theta}{2} \right] \tag{13}$$

$$u_y = \frac{K_I}{G} \sqrt{\frac{r}{2\pi}} \sin \frac{\Theta}{2} \left[2-2\nu - \cos^2 \frac{\Theta}{2} \right] \tag{14}$$

for plane strain.

Consider the vertical displacement u_y along the crack surface for which

$$\Theta = \pi$$

$$r = t$$

where t is a coordinate along the crack, starting at the crack tip. One should note to conform with usual practice, η replaces the displacement in y direction u_y. Recall from elasticity that:

$$G = \frac{E}{2(1+\nu)} \tag{15}$$

Substituting into Equations 12 and 14 the crack displacement for plane stress and plane strain can be written as

$$\eta = \frac{4K_I}{H} \left(\frac{t}{2\pi} \right)^{\frac{1}{2}} \tag{16}$$

$$K_I = \frac{\eta H}{4} \left(\frac{2\pi}{t} \right)^{\frac{1}{2}} \tag{17}$$

The equation holds only very near the crack tip

$$t \ll a$$

and allows one to calibrate K_I by measuring crack opening at a known distance very near the crack tip.

5. CRACK OPENING CALIBRATION

In order to find the slope with respect to the crack length $\partial\eta/\partial a$ of the crack opening profile, an approximation has been used. Orange (Reference 11) suggested a conic section approximation for a finite width edge cracked plate. This approximation is based on assuming a general conic section function for the crack opening shape and fitting the crack tip radius of curvature and crack mouth opening to determine the unknown coefficients. Further development of this relationship is presented in Appendix E. Following Orange and substituting for the crack tip curvature in terms of the stress intensity factor, using crack tip displacement equations, the following expression is derived:

$$\left(\frac{\eta}{\eta_o}\right)^2 = \frac{2}{2+\bar{m}}\left(\frac{t}{a}\right) + \frac{\bar{m}}{2+\bar{m}}\left(\frac{t}{a}\right)^2 \tag{18}$$

where η_o is the crack mouth displacement and $\bar{m}$ is the conic section coefficient.

$$\bar{m} = \pi\left[\frac{H\eta_o}{2\sigma a Y}\right]^2 - 2 \tag{19}$$

Y is a nondimensional stress intensity factor

$$Y = \frac{K_I}{\sigma\sqrt{a}} \tag{20}$$

Crack displacements of finite single edged cracked strips under bending or tension generated by Orange (Equation 18) were compared to the collocation method presented by Gross (Reference 20) and found to match within 3.2 percent. The Orange equation was compared to the Rice (Reference 3) solution for a center crack considering an infinite plate. The results were found to be exactly the same. The Orange equation was also used successfully by Grandt (References 6, 21) for cracks in fastener

holes and for radially cracked rings. Substituting the expression for Y Equation 20, and $\overline{m}$ Equation 19 into Equation 18, we obtain

$$\left(\frac{\eta}{\eta_o}\right)^2 = \frac{2}{\pi\left[\dfrac{H\eta_o}{2a^{\frac{1}{2}}K_I}\right]^2}\left(\frac{t}{a}\right) + \left[1 - \frac{8aK_I^2}{\pi H^2 \eta_o^2}\right]\left(\frac{t}{a}\right)^2 \tag{21}$$

$$\eta^2 = \left[\frac{8K_I^2}{\pi H^2}\right]t + \left[\frac{\eta_o^2}{a^2} - \frac{8K_I^2}{\pi H^2 a}\right]t^2 \tag{22}$$

In order to simplify the above equation,

let
$$B = \frac{8K_I^2}{\pi H^2} \tag{23}$$

and
$$R = \frac{\eta_o^2}{a^2} - \frac{8K_I^2}{\pi H^2 a} \tag{24}$$

Thus,
$$\eta = [Bt + Rt^2]^{\frac{1}{2}} \tag{25}$$

Also,
$$\frac{\partial \eta}{\partial a} = \frac{1}{2}[Bt + RT^2]^{-\frac{1}{2}} \cdot \frac{\partial}{\partial a}[Bt + Rt^2] \tag{26}$$
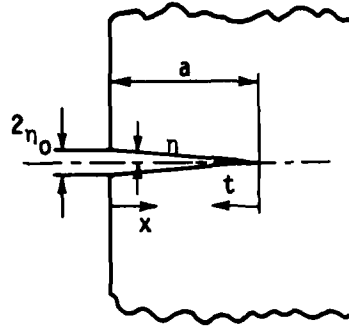
Figure 5. Edge Crack

From Figure 5, if $t = a-x$, then $\frac{\partial t}{\partial a} = 1$.

Thus,

$$\frac{\partial \eta}{\partial a} = \frac{1}{2} [Bt + Rt^2]^{-\frac{1}{2}} [\frac{\partial B}{\partial a} t + B + \frac{\partial R}{\partial a} t^2 + 2Rt] \qquad (27)$$

where:

$$\frac{\partial B}{\partial a} = \frac{16K_I}{\pi H^2} \frac{\partial K_I}{\partial a} \qquad (28)$$

and

$$\frac{\partial R}{\partial a} = \frac{8K_I^2}{\pi H^2 a^2} + \frac{2\eta_o}{a^2} \frac{\partial \eta_o}{\partial a} - \frac{2\eta_o^2}{a^3} - \frac{16K_I}{\pi H^2 a} \frac{\partial K_I}{\partial a} \qquad (29)$$

Equation 27 therefore defines $\partial \eta/\partial a$ in terms of the crack mouth displacement η_o and the stress intensity factor K_I and their derivative with respect to the crack length.

6. K_I FOR CASE 2

Substituting Equation 27 into Equation 10 and also changing the integration variable from x to t one obtains

$$K_{I_\text{②}} = \frac{H}{2K_{I_\text{①}}} \int_o^a p(t)_\text{②} [Bt+Rt^2]^{-\frac{1}{2}} [B + (\frac{\partial B}{\partial a} + 2R) t + \frac{\partial R}{\partial a} t^2] dt \qquad (30)$$

where B, R, $\frac{\partial B}{\partial a}$ and $\frac{\partial R}{\partial a}$ are defined previously and calculated for Case 1.

From Equation 30 it is clear that measuring the stress intensity factor K_I and the crack mouth opening η_o for various crack lengths and calculating their derivatives with respect to "a" allows one to construct the weight function for the Case 1 loading configuration. By knowing the stress distribution at the crack location for a noncracked body under the loading configuration of Case 2 $p(t)$②, one may obtain K_I for Case 2.

Computing this integral is quite tedious though possible for very simple forms of $p(t)$. However, numerical integration is possible for any $p(t)$ even if represented by a discrete numerical solution. In performing numerical integration, one should be cautioned to the fact that the weight function and therefore the whole expression under the integral is square root singular at the crack tip t=0 but still it can be shown that for the problems studied here a limit exists for the integral and, in most cases, the numerical integration converges quite rapidly.

SECTION III

EXPERIMENTAL TECHNIQUE

1. THE LASER INTERFEROMETRY METHOD

Stress intensity factor K calibrations obtained by measuring crack tip displacements require a technique capable of accurately measuring extremely small displacements very near the crack tip. As a rule of thumb, the relations for the crack tip displacement field as expressed in Equations 11 to 14 are regarded to be sufficiently accurate within a distance of a/20 or smaller from the crack tip, where a is the crack length. The laser interferometry technique described here was reported in References 9, 10, and 19 to measure displacements of 0.1 microns at a distance of 50 microns from the crack tip.

Results were reported leading to K_I values that varied up to 15 percent from the theoretical value (for individual points). Most of these deviations were attributed to the imperfect crack and material characteristics and not to measurement errors. The technique is basically similar to conventional interferometry but only measures in-plane displacements on the surface.

Two small indentations are placed with a diamond indentor on both sides of the crack near the crack tip. Those indentations are typically square based pyramids with a base length of 20 to 40 microns and located 50 microns apart on both sides of the crack (Figure 6). A laser coherent source impinges upon the indentations. The beam is diffracted back at an angle α_o with respect to the incident beam as shown schematically in Figure 7.

Since the indentations are placed close together, the respective diffraction beam overlaps resulting in interference fringe patterns on either side of the incident laser beam. A photograph of a typcial inter-ference pattern is shown in Figure 8.
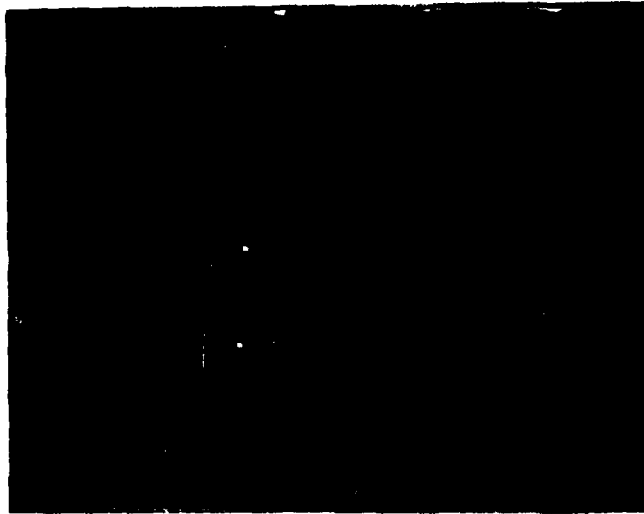
Figure 6. Surface Indentation (x280 Magnification)
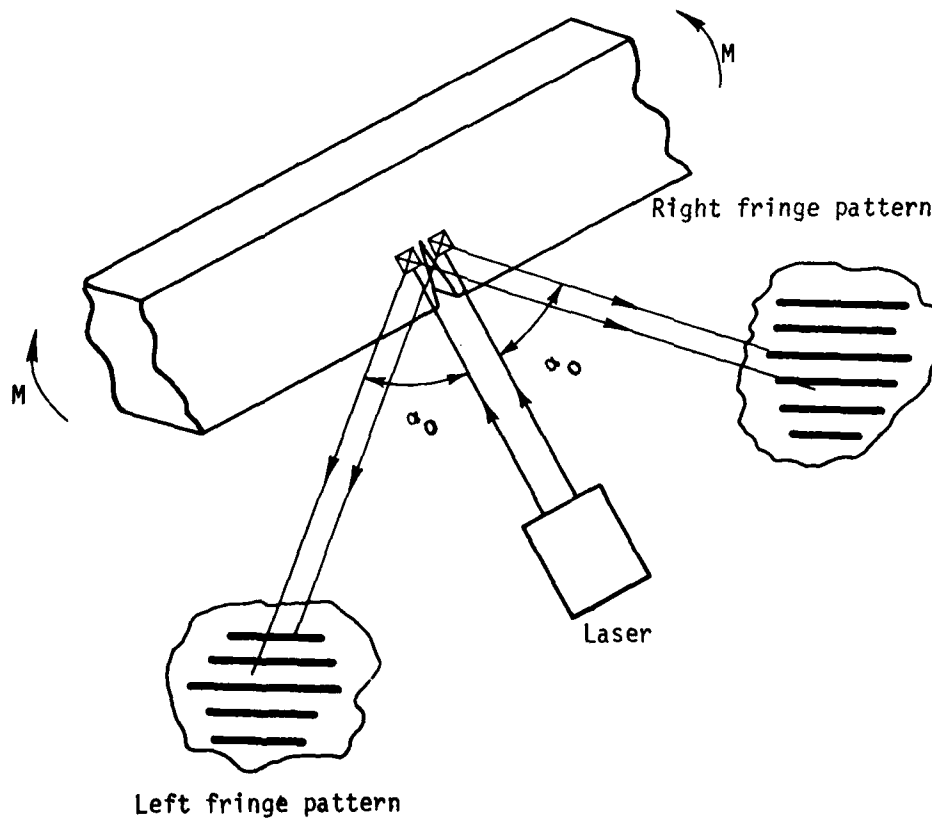
Figure 7. Schematic Showing Fringe Pattern Generation
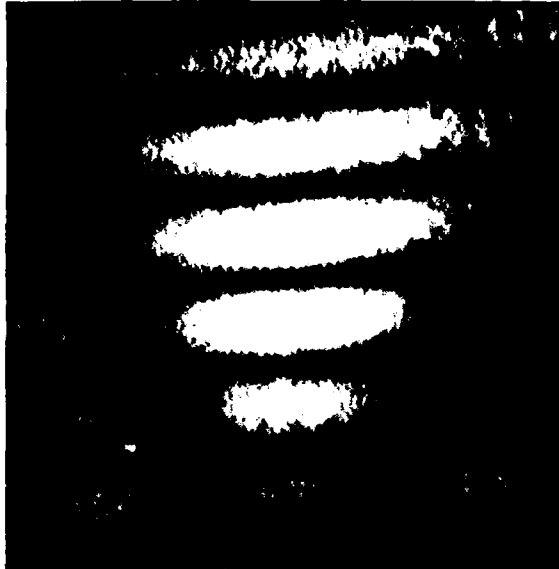
Figure 8. Typical Interference Fringe Pattern

The relation between the indentation spacing and the fringe order
is set by the following equation (Reference 9):

$$d \sin \alpha_o = m\lambda \qquad (31)$$

where d is the distance between indentations, λ is the wave length of
the source, and m is the fringe order.

As a load is applied to the specimen, the crack opens and the dis-
tance between the indentation changes. The relation between the change
in d and the change in the fringe order δm from a fixed point of view is

$$\delta d = \delta m \, \lambda/\sin \alpha_o \qquad (32)$$

Now observing the fringe pattern from a fixed point allows one to count
the number of fringes passing and hence determine the change in the
fringe order. Equation 32 will then give the change in the distance d
between the indentations that correspond to the crack opening. Averaging
the left and right fringe number will eliminate free body motion.

2. TEST APPARATUS

The test specimens used were flat strips of Aluminum 7075 T651. A small V notch was placed on the edge of the specimen to allow pre-cracking and a shallow groove was cut at the edge as to fit the clip gage used to measure crack mouth openings. (Figure 9).
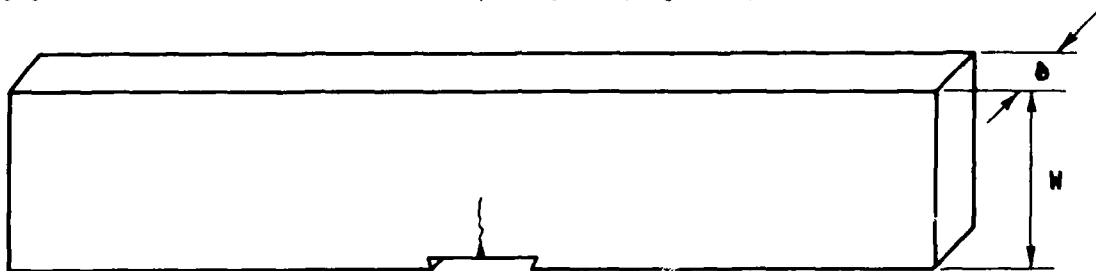
Figure 9. Test Specimen

The specimen was placed in a four-point bending fixture. Load was applied by a standard Instron machine equipped with a compression load cell (Figure 10).

Bending fixture

Specimen

Clip gage

Load cell
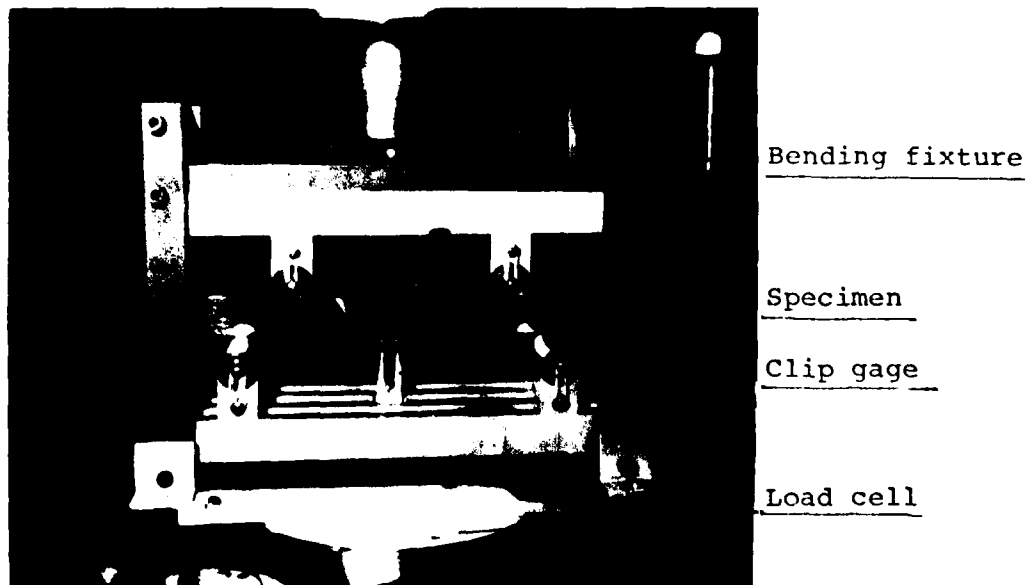
Figure 10. Specimen Set Up in Bending Fixture

The crack mouth opening was measured by a clip gage placed in the premachined groove. The clip gage consists of two small steel plates on which strain gages were bonded (Figure 11). Precalibrating the clip gage allows one to relate the mouth opening with the changes in strain measured.

Two pyramid-type indentations have been placed near the crack tip by a standard Lietz microhardener tester with a diamond indentor of a square based pyramid shape with face angles of 136 degrees. The indentations were impinged by a Spectra Physics Model 120 5 MW HeNe laser. The laser beam wave length λ was 0.6328 microns and had a divergence angle of 0.71 mr and a beam diameter of 0.57 mm. The laser was located so that the beam impinged perpendicular to the specimen surface. The angle of the diffracted beam α_0 can be calculated directly by knowing the face angle of the indentation. (Figure 11).
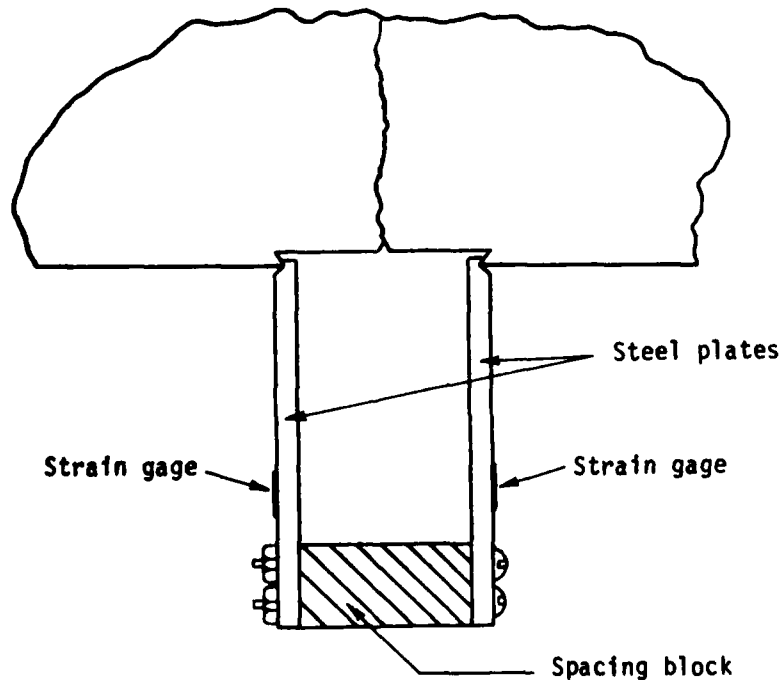
Figure 11. Clip Gage Setup

The fringes created by the interference of the reflected beams were picked up by two photoresistors that were located in a fixed place on the fringe pattern.

The active face of the photo resistors was masked leaving a narrow slit (smaller than the fringe spacing) to allow effective distinction between individual fringes. A photograph of the test apparatus is seen in Figure 13.

As load was applied and the fringes started moving, the photoresistor created an electrical signal that after proper amplification could be recorded with the aid of a strip chart recorder.

3. TEST PROCEDURE

Two Aluminum 7075 T651 specimens were each used to test 5-10 different crack lengths. The first specimen was used for longer cracks and the second for shorter cracks with some overlapping between the regions that allowed comparing between the two. The specimens were precracked in the long transverse (LT) direction of the material in three-point bending on a Schenck fatigue machine using cyclic loads at a frequency of 20 Hz. The precracking stress intensity factor varied from 6000-9000 psi $\sqrt{in}$. The higher K_I was used to initiate and propagate the crack to about 80 percent of the desired length, and the lower K_I levels were applied to get the final sharp crack.

Two indentations were placed on the surface 50-200 microns behind the crack tip as explained previously. A load of 200 grams on the indentor diamond head was found most suitable to create good reflecting indentations with a base square dimension of approximately 30 microns. The specimen was mounted on the loading fixture, and the two photo-resistor output signals together with the clip gage and load cell signals were monitored by a four-channel strip chart recorder to create a common time basis.

The specimens were loaded typically to values of K_I = 12-14 ksi $\sqrt{in}$ so the amount of plasticity in the specimen was kept small (Appendix B). Two load cycles were applied prior to actual testing so that the crack would appear to its full length on the surface and would easily be seen under a microscope.

20
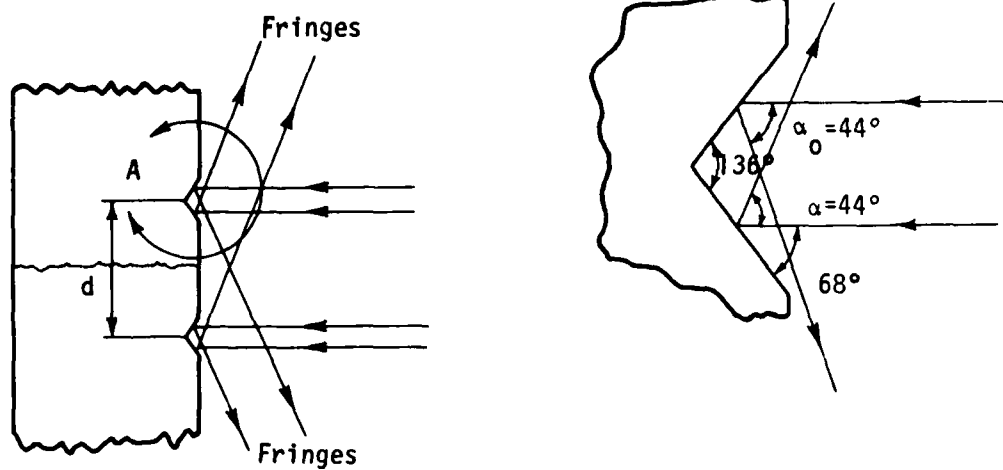
Figure 12. Laser Beam Reflection
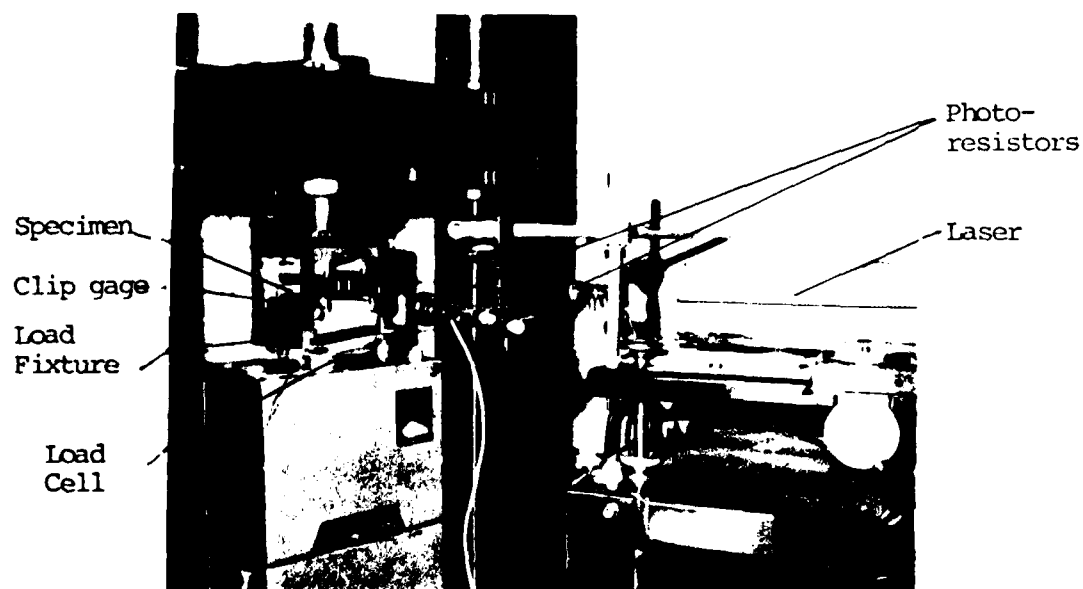
Figure 13. Test Apparatus Setup

During the preload cycle the photoresistors were relocated to a position such that the maximum fringe intensity could be observed. Since the photoresistors were fixed in position while the specimen with the indentation was displacing due to the applied load, it became necessary to establish the final location of the resistors under a mean load so that the indentations could still stay within the beam boundaries over the extreme deflection.

Three load cycles were applied to each specimen for each crack length. After each test the crack length was measured in order to account for any crack propagation during the test cycle. Then the crack was propagated to the next stage in the Schenck fatigue machine. In addition, for two different crack lengths the crack surface displacement was measured along the crack at 2-6 different locations using previously applied indentations in order to verify the Orange (Reference 11) conic section approximation for the crack opening.

SECTION IV

DATA REDUCTION AND NUMERICAL TECHNIQUE

1. K_I FOR CASE 1

The fringe patterns, crack mouth opening, and loads were all recorded on a four-channel strip chart recorder. A typical chart for a single loading cycle is shown in Appendix C, Figure C-1.

As explained previously, two sets of fringes were created by the reflected beam from the indentation. For each set of fringes, a slope of number of fringes per unit load $\delta m/p$ can be obtained. These slopes were averaged to eliminate free body motion. A more detailed description of the laser interferometer data reduction procedure can be found in Appendix C.

Using Equation 32

$$\frac{n}{P} = \frac{1}{2} \frac{\delta d}{P} = \frac{1}{P} = \frac{1}{2} \frac{\delta m}{P} \cdot \frac{\lambda}{\sin \alpha_o} \tag{33}$$

where $\lambda/\sin \alpha_o$ is the calibration factor of the interferometer used here. Equation 33 allows one to compute the displacement per unit load. The loading and unloading results of three loading cycles were averaged to give an average displacement per unit load. The distance t of the indentation behind the crack tip was computed by averaging the initial distance before the test with the one measured after three test cycles. Since only three cycles were applied and the amount of crack propagation was very small (a few microns), linear interpolation was adequate to give a sufficiently accurate estimate.

K_I for Case 1 can now be determined from the crack displacement near the crack tip (Equations 12 or 14). In most cases Θ is close enough to 180° so the simplified form of Equation 17 can be used.

Since the measurements are on the surface, the stress field should be considered as plane stress and H should be given the value of E (1×10^7 for aluminum 7075T651). Now Equation 17 takes the form

$$\frac{K_I}{P} = \left(\frac{\eta}{P}\right) \frac{E}{4} \left(\frac{2\pi}{t}\right)^{\frac{1}{2}} \tag{34}$$

This data will usually be converted to some nondimensional form.

2. CRACK MOUTH OPENING

The crack mouth opening η_0 was recorded directly from the clip gage readings. The crack mouth opening per unit load was then readily obtained from a η_0 versus P plot using only the linear part of the curve and neglecting the initial nonlinear part which is associated with crack closure effects.

3. NUMERICAL TECHNIQUE FOR K_I CASE 2 COMPUTATION

The rest of the computation, which involved calculating stress intensity factors for different Case 2 loadings were programmed and handled numerically. The $K_I \textcircled{1}$ data was fitted by a suitable interpolation curve. Interpolated values of $K_I \textcircled{1}$ and $\frac{\partial K_I \textcircled{1}}{\partial a}$ were computed for any desired crack length a/w. In a similar way, the crack mouth opening data for Case 1 $\eta_0 \textcircled{1}$ was fitted by an interpolating curve that allows one to compute values of η_0 and $\frac{\partial \eta_0}{\partial a}$ for the desired points. These interpolations are calculated in a different subroutine so any desired interpolation function can be tried without changing the main program. A comparison table for K_I and η_0 for interpolated data versus actual data is printed out so one can judge the accuracy of the interpolation process chosen. Fourth order least square polynomials will give reasonable results in many cases.

Using Orange (Reference 11) conic equation discussed in Appendix E for the crack opening profile, the derivative of the crack opening along the crack with respect to the crack length can be computed through Equation 27.

Since different factors are used to nondimensionalize the K_I and η_0 data, care should be taken to bring all the K_I, $\frac{K_I}{\partial a}$, η_0 and $\frac{\partial \eta_0}{\partial a}$ to a common basis. Using Equation 9, the weight function is

computed for each crack length at any point along the crack. The constant H is determined depending on plane stress or plane strain conditions (Appendix B). The stress distribution along the crack location for a noncracked body $p(t)$ is supplied by a separate subroutine and can be easily fitted with available data or some known analytical solution. K_I for Case 2 now is computed through integrating Equation 30.

The integral is performed numerically using a Romberg integration scheme (Reference 24). Although the weight function and thus the integrand in Equation 30 is singular at the crack tip, the integral will still converge to a distinct value quite rapidly for most $p(t)$ functions. Because of the crack tip singularity, the lower limit of this integral cannot be set to zero. A value close to zero should be taken and this value can be made smaller and smaller by an iterative process until the value of the integral converges within a specified accuracy.

Since the numerical integration process may be executed many times until convergence is obtained, an efficient algorithm should be used to reduce the required computer time. Romberg integration scheme used here is a powerful and efficient numerical integration technique. It is based upon the trapezoidal rule combined with Richardson extrapolation. More details of this scheme can be found in Hornbeck (Reference 24). Using this scheme reduced the computer time by a factor of about 200 compared to the Simpson's rule integration scheme. A detailed description of the computer program is presented in Appendix D.

SECTION V

EXPERIMENTAL RESULTS

1. EXPERIMENTAL MEASUREMENTS

Two Aluminum 7075 T651 edge cracked strips were used in the experiments. The specimens were cut out from a rolled plate and the crack was grown in the long transverse (LT) direction of the material.

The dimensions of the specimens and the region of crack length in which they were tested are shown in Figure 14.
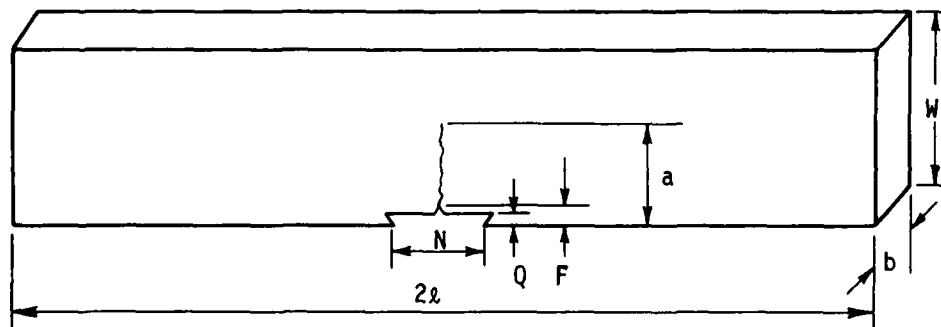
	2ℓ	b	w	N*	Q	F	a
Specimen A	9"	0.24"	1"	.27"	0.04"	0.05"	0.2328" -0.7517"
Specimen B	9"	0.245"	0.7885"	.31"	0.036"	0.036"	0.08153"-0.3753"

*N dimension determined for clip gage purposes

Figure 14. Specimen Dimensions

26

Specimen A was tested with ten different crack lengths with crack length to width ratios ranging from .2328-.7517. Specimen B was tested with five different crack lengths where a/w ranged from .1034-.476. Both specimens were loaded in a four-point bending fixture as shown in Figure 15.
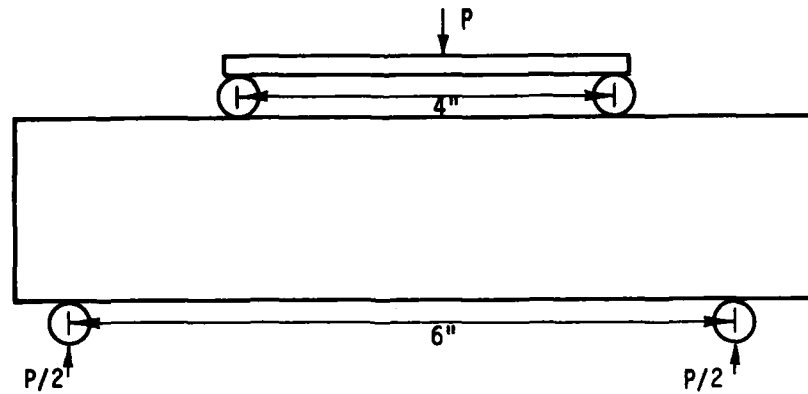
Figure 15. Loading Fixture Dimension

Each specimen was loaded through three loading cycles, and near crack tip displacement (by laser interferometry) and crack mouth openings were recorded. Table 1 represents the average results for all crack lengths measured.

2. DATA INTERPOLATION

The stress intensity data calculated from the interferometry measurements was converted to a nondimensional form of

$$\frac{K_I}{\sigma\sqrt{\pi a}} = \frac{K_I bW^2}{6M\sqrt{\pi a}} \tag{35}$$

where M is the bending moment $M = \frac{P \cdot 1''}{2}$.

The crack mouth opening data was converted to a nondimensional form

$$\frac{\eta_o}{2\sigma a} \cdot H = \frac{\eta_o bW^2 H}{12Ma} \tag{36}$$

TABLE 1

EXPERIMENTAL MEASUREMENT RESULTS

Specimen	Nondimensional crack length	Distance of indentation from crack tip	No of fringes per unit load	Crack mouth displacement per unit load
	a/w	r	$\delta m/p$	η_o/p
		Microns	$1/\ell b \times 10^{-3}$	$in/\ell b \times 10^{-6}$
B	.1034	101	5.093	0.568
B	.1586	83.5	6.623	0.7453
B	.2064	88	7.6713	0.9836
A	.2328	121.5	7.3128	0.856
B	.2646	86.5	9.116	1.268
A	.2666	99.5	7.580	1.14
A	.3094	143	10.180	1.405
A	.346	56	7.340	1.705
A	.3978	72	9.140	2.358
A	.436	46.5	8.0146	2.727
B	.476	47	12.808	4.121
A	.4893	50	10.130	3.6585
A	.5780	111.5	18.354	6.04
A	.6467	74	20.460	9.216
A	.7517	70	35.500	20.681

The nondimensional data for K_I and η_0 was interpolated by a least square fourth order polynomial. Table 2 and Table 3 present the actual experimental and the interpolated data for K_I (nondimensional) and η_0 (nondimensional) respectively including the relative difference in percent of the interpolating polynomial at the test point.

Figure 16 presents the actual experimental nondimensional K_I compared to the known reference results from Tada (Reference 12). Figure 17 presents the actual experimental nondimensional data for η_0 compared to the known reference results from (Reference 12). The average difference between the reference values of K_I and the experimental data is 6% while the maximum difference for a single measurement is up to 14%. These results are similar in accuracy to the ones obtained by Macha (Reference 10) for the laser interferometry technique. The values of K_I from the interpolating polynomial that were actually used to compute the weight function are similar in accuracy with a maximum difference of 13% and an average difference of 6% compared to Reference 12. One should note that the relatively large difference in the slope of $\frac{\partial K_I}{\partial a}$ for some of the short crack lengths (Figure 16) will have only a minor influence on the weight function computation as can be seen from examining Equation 30. η_0 data as well as the interpolating polynomial fits the Reference 12 values much better as seen in Figure 17.

3. CRACK PROFILE MEASUREMENTS

For two different crack lengths on specimen A the crack opening was measured along the crack at several points in addition to the point near the crack tip and at the crack mouth. These measurements were done by the laser interferometry technique. The existing indentations left behind as the crack propagated were used for these measurements. The crack openings along the crack were compared to the Orange (Reference 11) conic sections and found to match this approximation excellently (Figures 18 and 19).

TABLE 2

K_I (NONDIMENSIONAL) COMPARISON OF ACTUAL DATA TO
INTERPOLATED DATA

Crack Length	Actual K_I	Interpolated K_I	Relative Difference in %
a/W	$\dfrac{K_I bW^2}{\sigma M\sqrt{\pi a}}$	$\dfrac{K_I bW^2}{\sigma M\sqrt{\pi a}}$ *	
.1034	.9073	.9467	4.34
.1586	1.0575	.9776	-7.56
.2064	1.0572	1.0545	-.26
.2328	1.1137	1.1060	-.69
.2646	1.1007	1.1705	6.35
.2666	1.1862	1.1746	-.98
.3096	1.2366	1.2590	1.81
.3460	1.3490	1.3244	-1.82
.3978	1.3804	1.4086	2.04
.4360	1.4388	1.4696	2.14
.4760	1.5646	1.5424	-1.42
.4893	1.6551	1.5710	-5.08
.5780	1.8481	1.8774	1.59
.6467	2.3460	2.3688	.97
.7517	3.9513	3.9413	-.25

*The interpolating polynomial is:

$$\frac{K_I bW^2}{\sigma M\sqrt{\pi a}} = 70.75(a/W)^4 - 92.45(a/W)^3 + 42.95(a/W)^2 - 6.53(a/W) + 1.257$$

TABLE 3

η_o (NONDIMENSIONAL) COMPARISON OF ACTUAL DATA TO
INTERPOLATED DATA

Crack Length	Actual η_o	Interpolated η_o	Relative Difference in %
a/W	$\dfrac{\eta_o bW^2 H}{12Ma}$	$\dfrac{\eta_o bW^2 H}{12Ma}$ *	
.1034	1.9440	1.9500	.31
.1586	1.6643	1.6491	-.91
.2064	1.6855	1.6334	-3.09
.2328	1.6163	1.6879	4.43
.2646	1.6950	1.7933	5.80
.2666	1.8796	1.8011	-4.18
.3096	1.9961	1.9923	-.19
.3460	2.1660	2.1823	.75
.3978	2.6055	2.4945	-4.26
.4360	2.7493	2.7696	.74
.4760	3.0632	3.1251	2.02
.4893	3.2866	3.2648	-.66
.5780	4.5933	4.6431	1.08
.6467	6.6244	6.5725	-.78
.7517	12.0980	12.1082	.08

*The interpolating polynomial is:

$$\frac{\eta_o bWH}{12Ma} = 210.38(a/W)^4 - 282.57(a/W)^3 + 150.74(a/W)^2 - 32.16(a/W) + 3.952$$
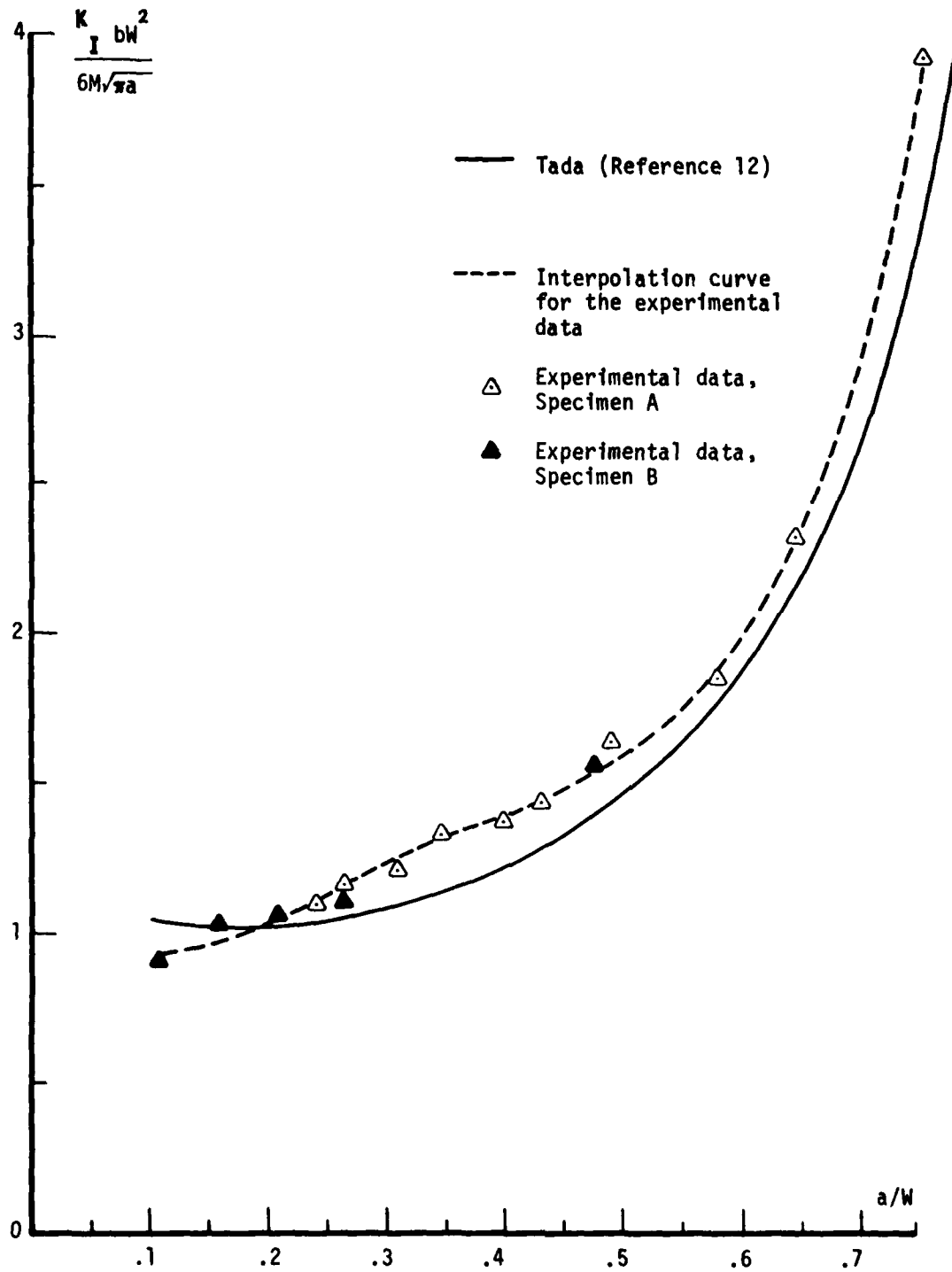
Figure 16. Stress Intensity Factor (Nondimensional) for Pure Bending
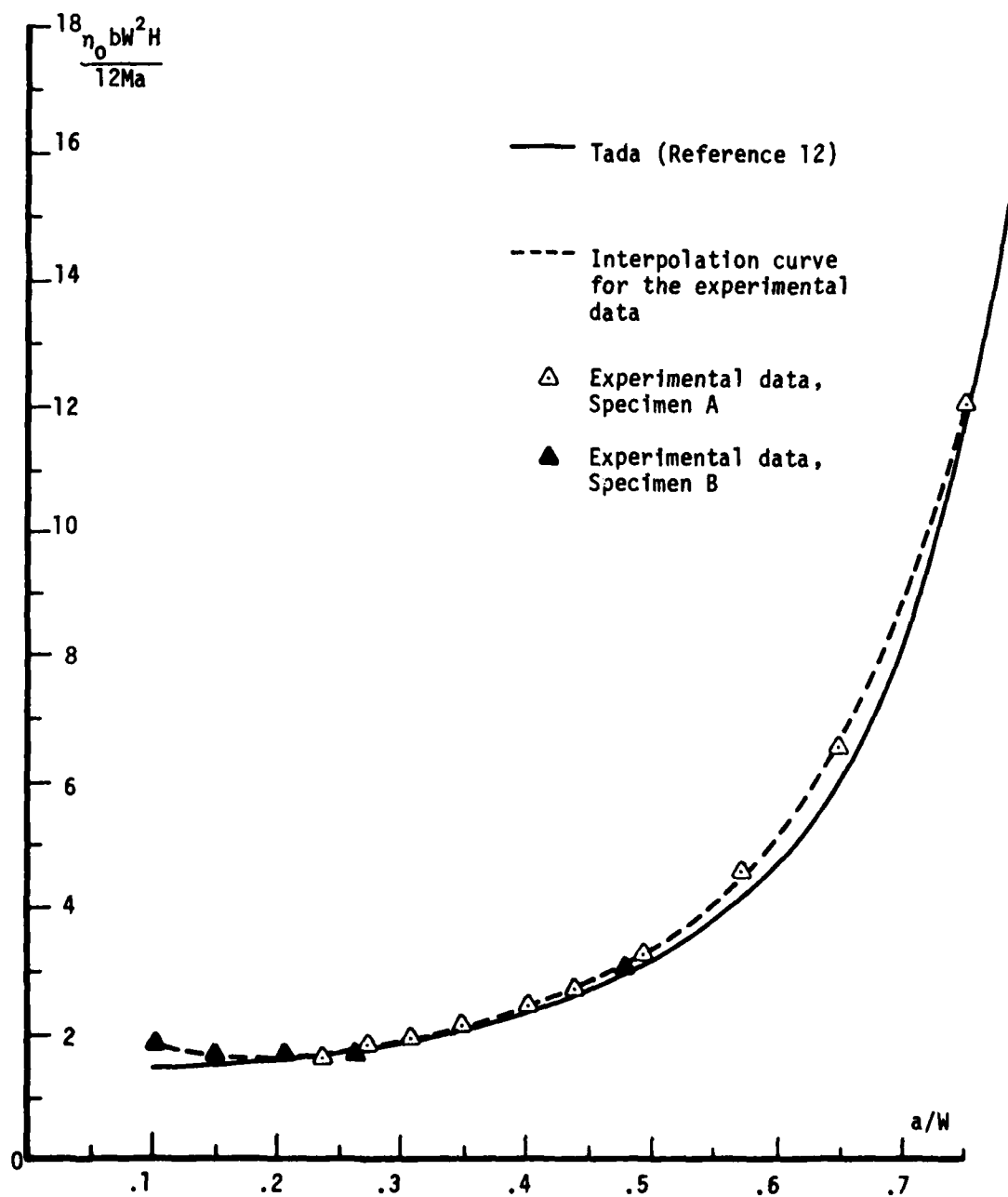
Figure 17. Crack Mouth Opening (Nondimensional) for Pure Bending
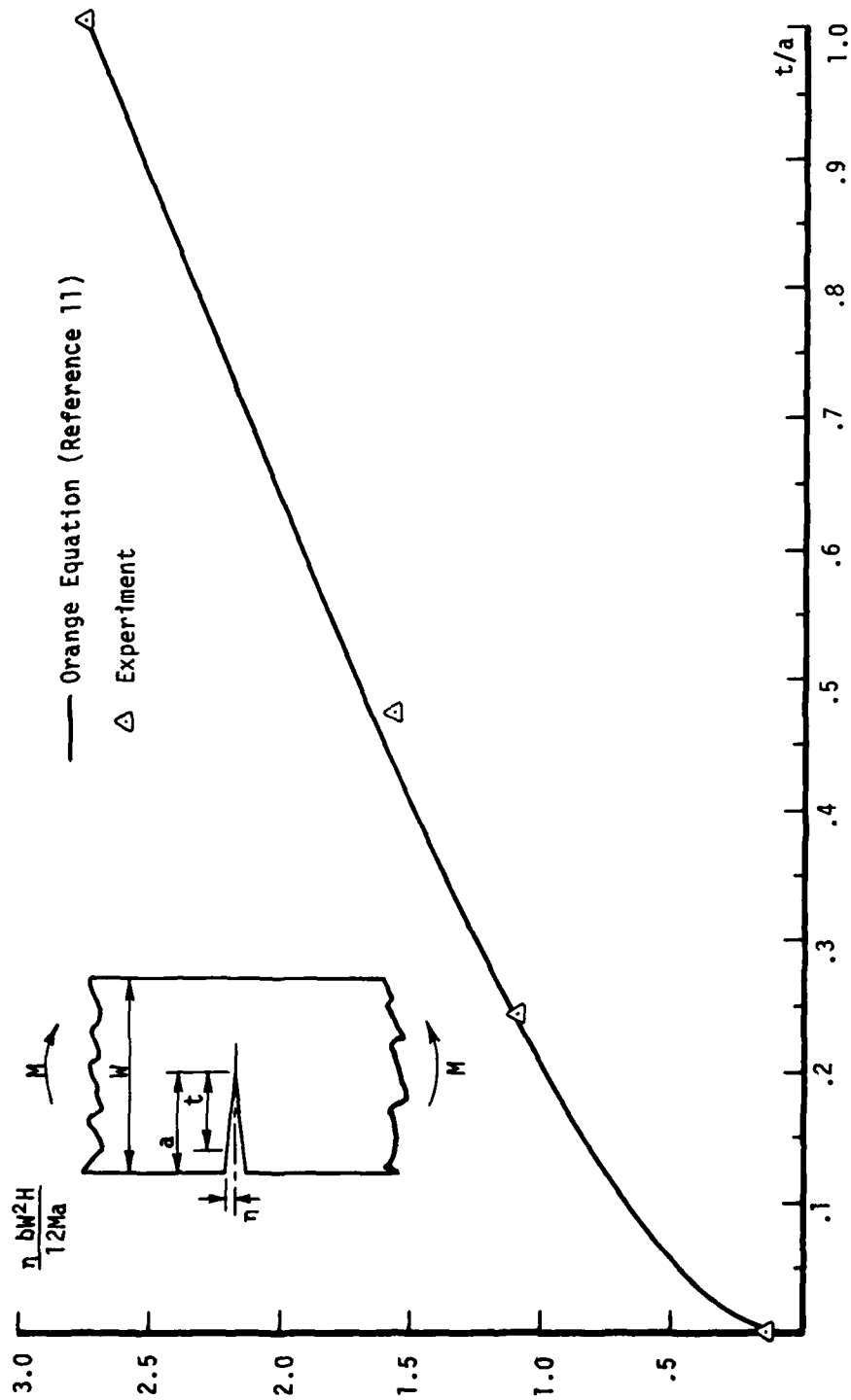
Figure 18. Nondimensional Displacement Along Crack Surface Compared to Orange Equation (Reference 11) Pure Bending a/W=0.436
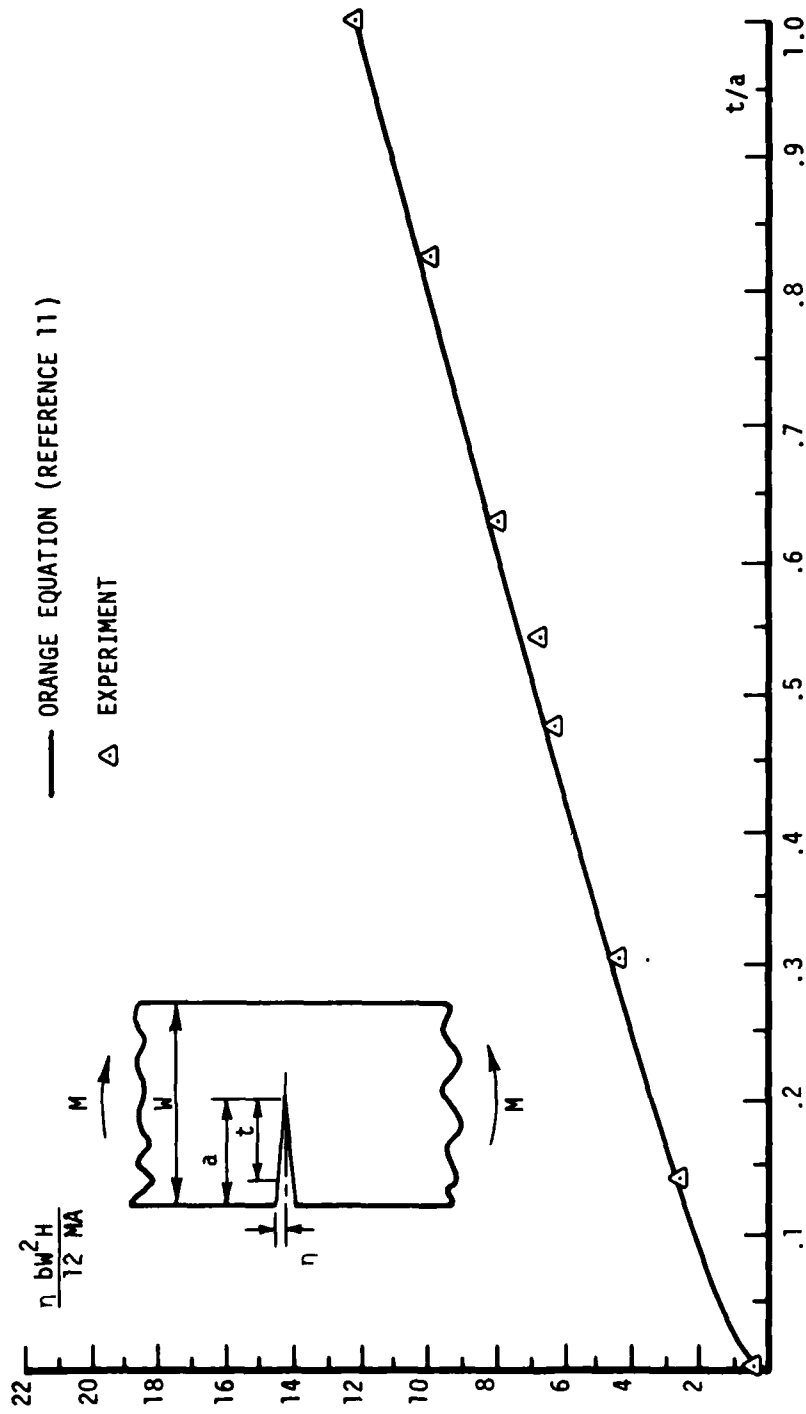
Figure 19. Nondimensional Displacements Along Crack Surface Compared to Orange Equation (Reference 11) Pure Bending, a/W=0.7517

4. CASE 2 LOADINGS

Three different loading configurations were chosen for Case 2, uniform tension, three-point bending with S/W of 4 and 8 (Figure 20). Each of the different Case 2 loading configurations requires another function p(t) as the noncracked body stress at the crack location stresses.
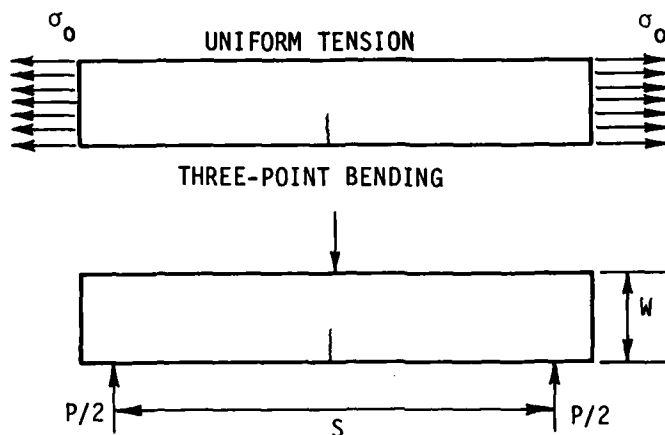
Figure 20. Case 2 Loading Configurations

5. UNIFORM TENSION

In this case,

$$p(t) = const. = \sigma_0 \tag{37}$$

where σ_0 is the remote stress. Since the standard nondimensional representation for K_I for uniform tension is

$$\frac{K}{\sqrt{\pi a}\sigma_0} \tag{38}$$

the function p(t) should be factored by $1/\sqrt{\pi a}\sigma_0$ to get K_I in the desired form. Therefore, take

$$p(t) = \frac{1}{\sqrt{\pi a}} \tag{39}$$

(in the computer program $1/\sqrt{\pi a}$ is already factored in the weight function so p(t) is substituted as 1.).

The results of the nondimensional stress intensity factor for uniform tension at equally spaced points from a/W=.1 to a/w=.7 are presented in Table 4. These results are compared to Tada's (Reference 12) solution. The results agree with the reference solution within 8 percent.

Figure 21 compares the reference solution (Reference 12) to the values calculated at the same a/W points where experiments were performed on the four-point bending specimen. One can see that the last point is the only calculated value that does not agree favorably with the reference data. Since the computations required differentation of experimental data, one should be very suspicious about the results obtained at the experimental interval end points. Close to the end points computing derivatives actually requires extrapolations that can be very inaccurate, since the behavior of the function is unknown in these regions.

Investigating Equation 30 shows clearly that the derivatives $\partial K/\partial a$ and $\partial \eta_0/\partial a$ have a relatively larger influence on the value of the weight function at longer crack lengths; therefore, the computed values are more likely to get distorted at the upper limit of the experimental a/W interval as can indeed be seen in Figure 21.

6. THREE-POINT BENDING

A solution for the stress distribution of a noncracked strip under three-point bending in a cross-section through the center is given by Timoshenko (Reference 27):

$$\sigma_x = \frac{3P}{2c^3 b} \left(\frac{\ell}{2} - \frac{c}{\pi} \right) y + \frac{P}{2\pi cb} + \frac{P}{\pi cb} \left(\frac{y^3}{2c^3} - \frac{?}{10} \frac{y}{c} \right) \qquad (40)$$

TABLE 4

K_I (NONDIMENSIONAL) FOR UNIFORM TENSION

Crack Length a/W	$\dfrac{K_I}{\sigma\sqrt{\pi a}}$ Calculated Using the Weight Function	$\dfrac{K_I}{\sigma\sqrt{\pi a}}$ From Ref 12	Relative Difference in %
.1000	1.2705	1.1957	6.26
.1500	1.2697	1.2682	.12
.2000	1.4041	1.3667	2.74
.2500	1.5540	1.4941	4.01
.3000	1.6855	1.6551	1.83
.3500	1.8170	1.8565	-2.13
.4000	1.9967	2.1080	-5.28
.4500	2.2917	2.4241	-5.46
.5000	2.7719	2.8266	-1.93
.5500	3.4752	3.3486	3.78
.6000	4.3636	4.0432	7.92
.6500	5.3158	4.9993	6.33
.7000	5.1832	6.3755	-3.02
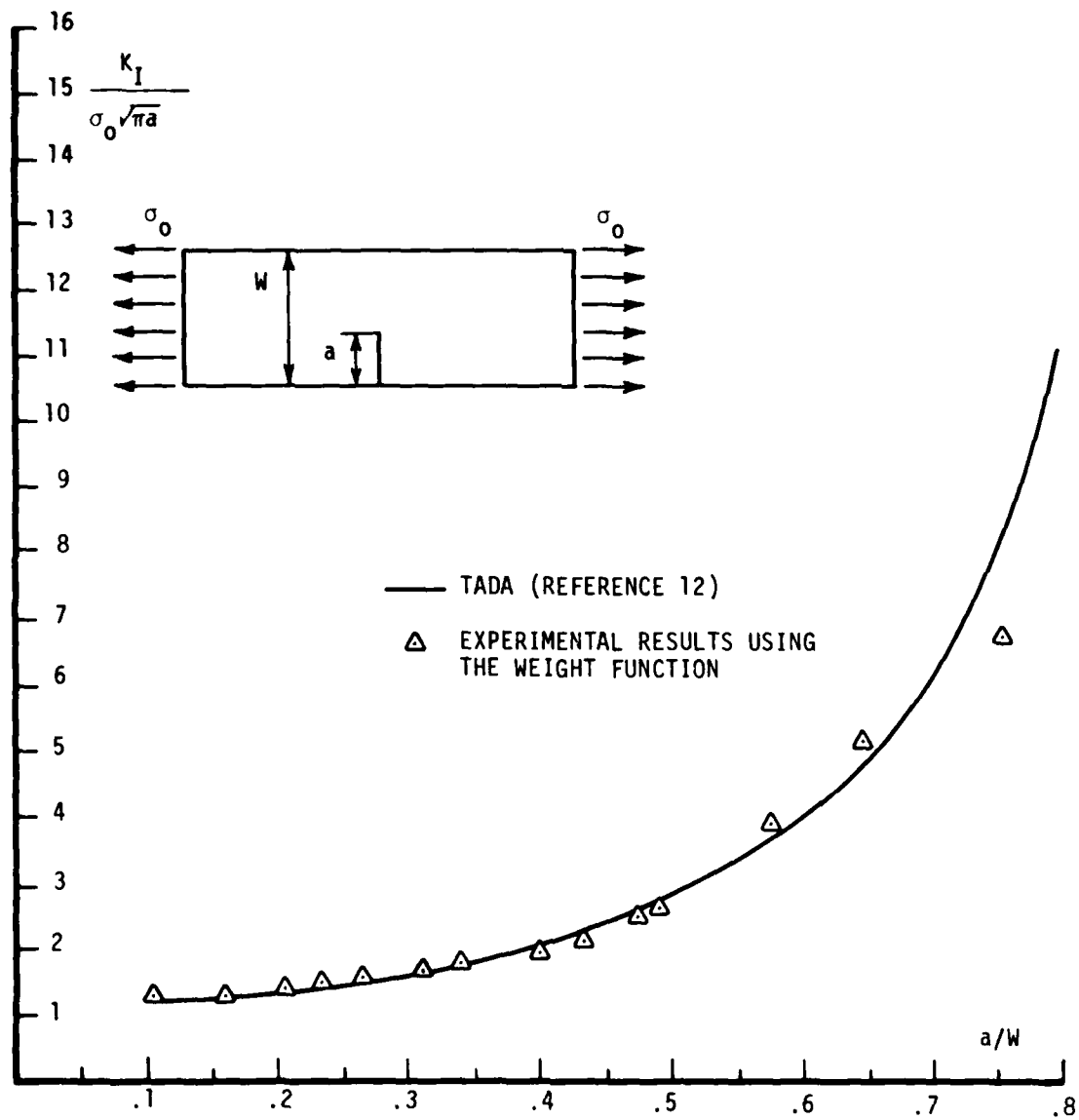
Figure 21.   Stress Intensity Factor (Nondimensional) for Uniform Tension

The terms of this equation are defined in the following Figure 22. σ_x is the stress in x-direction along AD.
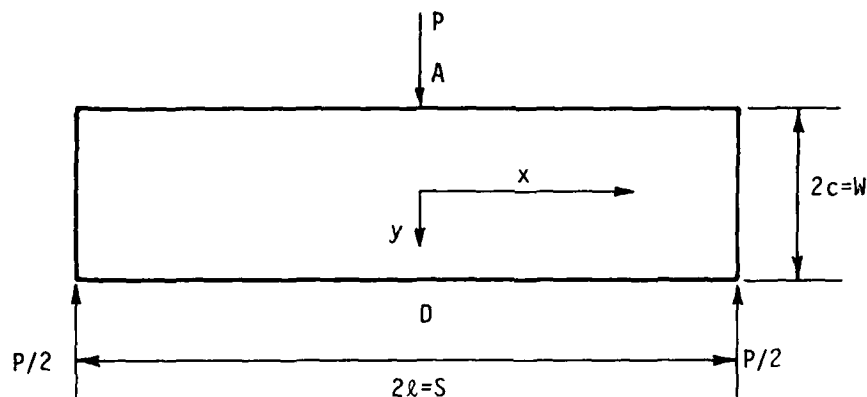
Figure 22. A Uniform Strip Under Three-Point Bending

According to Timoshenko, this expression gives the stress with very good accuracy except for point D where an error of $.121 \frac{P}{cb}$ *exists based on a more accurate solution.* This term will lead in our worst case to an error of 4 percent in the load distribution at the crack mouth location, but since, at this point the weight function has its lowest value, the integral of the product of h and p(t) is expected to have much better accuracy. The standard nondimensional solution is of the form

$$\frac{K_I}{\sigma \sqrt{\pi a}} \tag{40a}$$

where

$$\sigma = \frac{6M}{4bc^2} \quad \text{and} \quad M = \frac{P\ell}{2}$$

So the undimensional form of K_I becomes

$$\frac{K_I}{\sqrt{\pi a}} \frac{4c^2 b}{3P\ell} \tag{41}$$

The factor $1/\sqrt{\pi a}$ is already included in our computer program in the weight function so the form of $p(t)$ that is required in order to get K_I in the form of Equation 41 is

$$p(t) = \frac{\sigma_x(t)\, 4bc^2}{3P\ell} \tag{42}$$

Substituting Equation 40 to Equation 42 yields

$$p(y) = \frac{2}{3\pi}\left(\frac{c}{\ell}\right) + \left[1 - \frac{12}{5\pi}\left(\frac{c}{\ell}\right)\right]\frac{y}{c} + \frac{2}{3\pi}\left(\frac{c}{\ell}\right)\left(\frac{y}{c}\right)^3 \tag{43}$$

where $S = 2\ell$

and $W = 2c$

Changing to crack tip coordinates t the expression for y/c becomes

$$y/c = \frac{1}{(W/2)}\left(t + \frac{W}{2} - a\right) = 2\left(\frac{t}{W} - \frac{a}{W}\right) + 1 \tag{44}$$

Substitute Equation 44 into Equation 43 and get

$$p(t) = \frac{2}{3\pi}\left(\frac{S}{W}\right) + \left[1 - \frac{12}{5\pi}\left(\frac{S}{W}\right)\right]\left[2\left(\frac{t}{W} - \frac{a}{W}\right) + 1\right] + \frac{2}{3\pi}\left(\frac{S}{W}\right)\left[2\left(\frac{t}{W} - \frac{a}{W}\right) + 1\right]^3 \tag{45}$$

Results for the nondimensional stress intensity factor considering three-point bending (S/W=4 and S/W=8) are presented in Tables 5 and 6 respectively. These results are compared with known results from References 12 and 28. The reference solution claims to be accurate for a/W <.6 and in this interval the calculated experimental values are within 6.15 percent accuracy for S/W=4 and 5.9 percent for S/W=8.

Figures 23 and 24 show the calculated K_I for three-point bending for the a/W points where actual data was gathered for the four-point bending. As for the uniform tension case, the last point is the only one not fitting the expected curve because of the inaccurate extrapolation procedure explained previously.

TABLE 5

K_I (NONDIMENSIONAL) FOR THREE-POINT BENDING, S/W=4

Crack Length a/W	K_I (Nondimensional) Calculated Using the Weight Function	K_I (Nondimensional) Ref 28	Relative Difference in %
.1000	1.0134	.9849	2.89
.1500	.9447	.9731	-2.91
.2000	.9838	.9803	.36
.2500	1.0272	1.0037	2.34
.3000	1.0491	1.0425	.64
.3500	1.0635	1.0979	-3.13
.4000	1.1015	1.1736	-6.15
.4500	1.1994	1.2754	-5.96
.5000	1.3866	1.4112	-1.74
.5500	1.6656	1.5910	4.69

TABLE 6

K_I (NONDIMENSIONAL) FOR THREE-POINT BENDING, S/W=8

Crack Length a/W	K_I (Nondimensional) Calculated Using the Weight Function	K_I (Nondimensional) Ref 28	Relative Difference in %
.1000	1.0630	1.0156	4.66
.1500	.9911	1.0080	-1.68
.2000	1.0314	1.0183	1.28
.2500	1.0755	1.0438	3.04
.3000	1.0964	1.0839	1.15
.3500	1.1087	1.1403	-2.77
.4000	1.1450	1.2167	-5.89
.4500	1.2431	1.3189	-5.75
.5000	1.4328	1.4549	-1.52
.5500	1.7160	1.6349	4.96
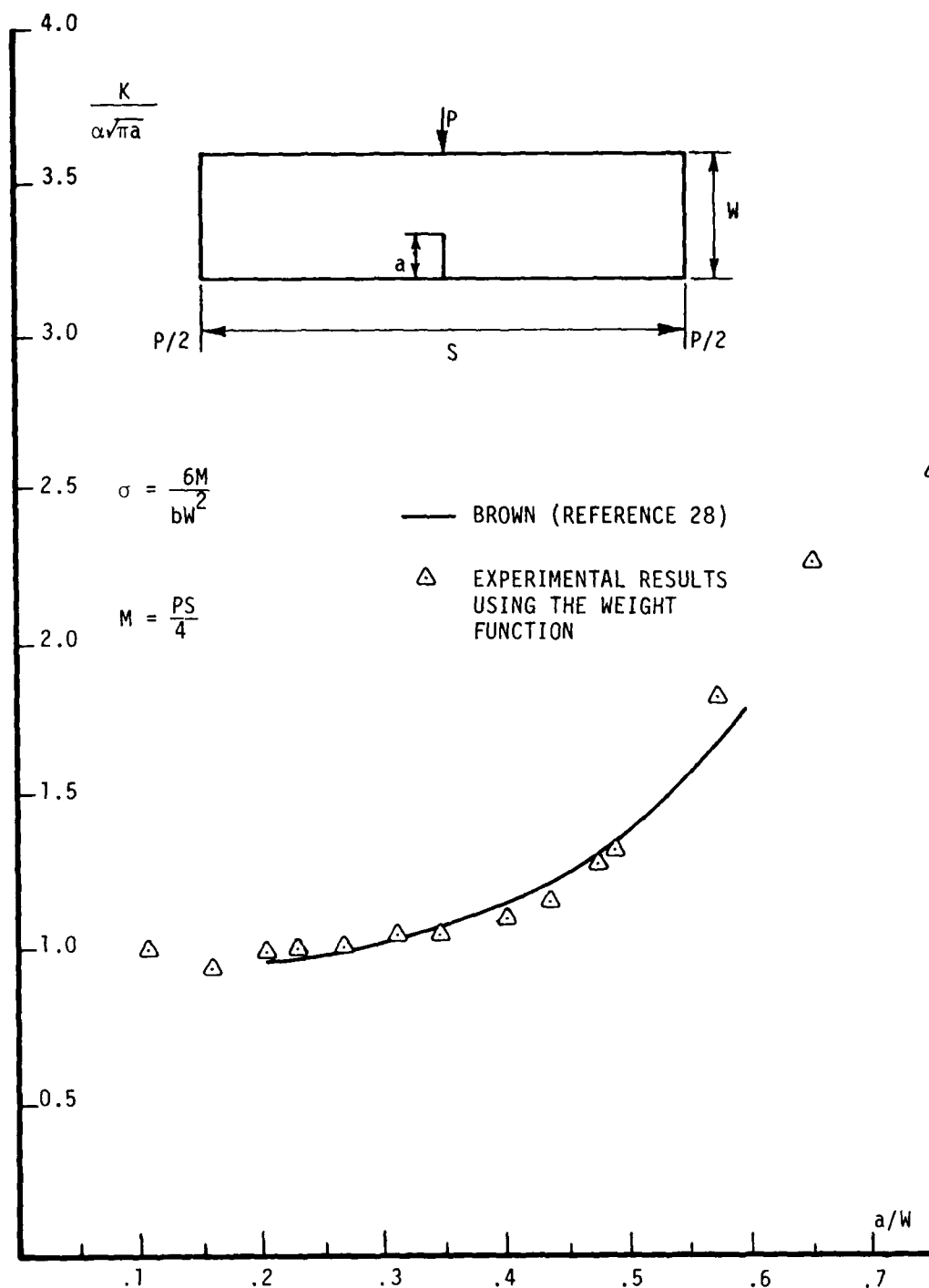
Figure 23. Stress Intensity Factor (Nondimensional) for Three-Point
Bending S/W=4
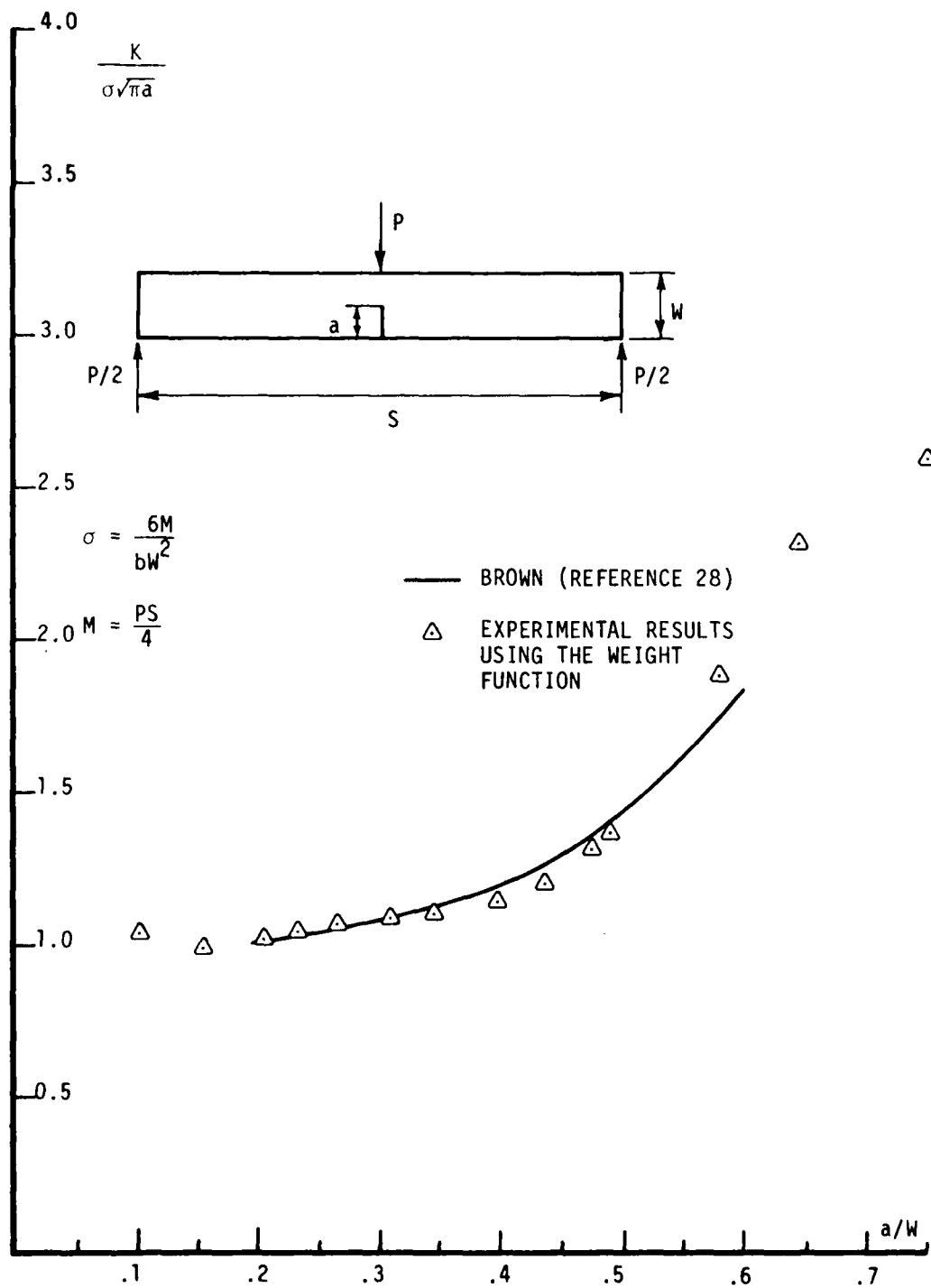
Figure 24.   Stress Intensity Factor (Nondimensional) for Three-Point
Bending, S/W=8

SECTION VI

CONCLUSIONS

1. This work shows clearly that the experimental weight function procedure leads to excellent results for the stress intensity factor without actually testing the loading configuration in question.

2. A set of experiments of a single loading configuration can be used to calculate the stress intensity factor solution for any other loading configuration applied to the same geometry. The only additional information required is the stress distribution at the crack location for a <u>noncracked body</u>.

3. One should limit the results obtained for a different loading only to the same a/W region studied in the original experiment. Extrapolations, or even calculations, near the test a/W limits may lead to inaccurate results.

4. Because data scatter can lead to errors when differentiated, care should be taken to collect enough data to yield reasonable interpolating functions.

5. Even though some error was introduced in the K_I and η_o measurements, the numerical procedure using the derivatives of K_I and η_o did not distort the Case 2 results beyond the basic accuracy of the Case I measurements.

6. The laser interferometric technique provides an efficient procedure for crack opening measurements and leads to accurate results for this type of measurement.

7. The Orange (Reference 11) conic section again provided an accurate representation for the crack opening profile for edge cracked strips. This conic section should, however, be compared with actual profile measurements (as done here) prior to applying it to other geometries.

8. The fact that the actual cracks were not perfectly straight on a micro-scale, as assumed in this theory, is the most likely source for K_I calibration errors for Case 1 loading (four-point bending). Perhaps other materials would give "straighter" cracks which more closely match the analytical behavior.

APPENDIX A

THE WEIGHT FUNCTION

The idea of the weight function has been introduced by Bueckner (Reference 2) and was also discussed in References 2 through 8.

The following analysis shows that if the complete solution of the stress intensity factor and the crack opening displacement for a crack subjected to a certain loading system is known, then the stress intensity factor solution for the geometry under another loading configuration may be obtained directly from the known solution.

Let us consider a cracked body with loads $P_1,\ldots,P_n$ as described in Figure A-1.
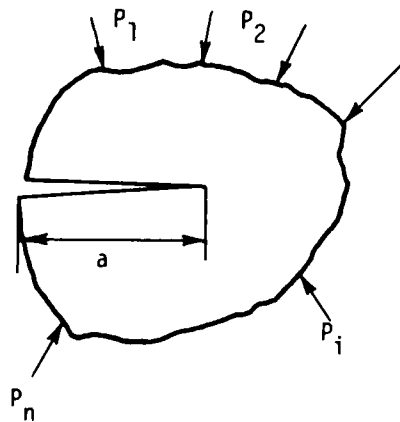
Figure A-1. Loaded Cracked Body

The elastic energy release rate, often referred to as the Griffith energy rate, can be defined following Irwin (Reference 22) as

$$\mathcal{G} = \left. \frac{\partial U}{\partial a} \right|_P \tag{A-1}$$

where U is the total potential energy stored in the cracked body and a is the crack length.

g has units of force and is often referred to as the crack extension force

$$U = \frac{1}{2} \sum_{i=1}^{N} \sum_{j=1}^{N} C_{ij} P_i P_j \tag{A-2}$$

where C_{ij} is the compliance coefficient defined as the deflection at point i due to a unit force at point j.

$$\mathcal{G} = \left. \frac{\partial U}{\partial a} \right|_P = \frac{1}{2} \sum_{i=1}^{N} \sum_{j=1}^{N} \frac{\partial C_{ij}}{\partial a} P_i P_j = \frac{1}{2} \sum_{i=1}^{N} \frac{\partial u_i}{\partial a} \cdot P_i \tag{A-3}$$

where

$$u_i = \sum_{j=1}^{N} u_i^j = \sum_{j=1}^{N} C_{ij} P_j \tag{A-4}$$

u_i^j is the displacement at i due to load P_j.

Since the elastic energy release rate g (based on strain energy consideration) and the stress intensity factor K (based on crack tip stress considerations) are both parameters that characterize crack growth, a relation can be established between them as shown by Hertzberg (Reference 15).

$$\mathcal{G} = \frac{K^2}{H} \tag{A-5}$$

where H is defined as

$$H = \begin{cases} E & \text{for plane stress} \\ \dfrac{E}{1-\nu^2} & \text{for plane strain} \end{cases} \qquad (A-6)$$

Since K is the linear elastic stress intensity factor, superposition can be used to write

$$K = \sum_{i=1}^{N} K_i = \sum_{i=1}^{N} k_i(a) P_i \qquad (A-7)$$

k_i stress intensity factor per unit load. Substituting, into the elastic energy release rate

$$\mathcal{G} = \frac{K^2}{H} = \frac{1}{H} \sum_{i=1}^{N} \sum_{j=1}^{N} k_i(a) k_j(a) P_i P_j \qquad (A-8)$$

By equating Equation A-8 to Equation A-3 we conclude that they should be equal term by term.

Thus,

$$\frac{k_i(a) k_j(a)}{H} = \frac{1}{2} \frac{\partial C_{ij}(a)}{\partial a} \qquad (A-9)$$

If the full solution for K is known only for one load, say P_m, then

$$k_i(a) = \frac{H}{2} \frac{\partial C_{im}(a)}{\partial a} \cdot \frac{1}{k_m(a)} \qquad (A-10)$$

recall, that we defined in Equation A-7 $k_m = \dfrac{K_m}{P_m}$

and in Equation A-4 $C_{im} = \dfrac{u_i^m}{P_m}$

Therefore,

$$k_i(a) = \frac{H}{2} \frac{\partial u_i^m}{\partial a} \frac{1}{K_m} \qquad \text{(A-11)}$$

and since

$$K = \sum_{i=1}^{N} k_i(a) P_i \qquad \text{(A-12)}$$

Then

$$K = \frac{H}{2K_m} \sum_{i=1}^{N} \frac{\partial u_i^m}{\partial a} P_i \qquad \text{(A-13)}$$

For an arbitrary distribution of P_i, and a set of surface tractions $T(s)$, the expression for K can be written as

$$K = \frac{H}{2K_m} \int_S \frac{\partial u^m}{\partial a} (s,m) \, T(s) \, ds \qquad \text{(A-14)}$$

If one defines the weight function as

$$h_m(s,a) = \frac{H}{2K_m(a)} \frac{\partial u^m(s,a)}{\partial a} \qquad \text{(A-15)}$$

Then we can readily see that the weight function depends only on the geometry of the cracked body (including the crack length) and the loading configuration denoted by the superscript m.

Substituting the term for the weight function into Equation A-14, we get

$$K = \int_s h_m(s,a)T(s)ds \qquad (A-16)$$

We can therefore conclude that the stress intensity factor for the arbitrary surface traction T(s) can be obtained from the known weight function we computed considering the loading configuration m. In a little bit more general derivation, the body forces can be included and one can write

$$K = \int_\Gamma T \cdot h d\Gamma + \int_A f \cdot h \cdot dA \qquad (A-17)$$

where h is the weight function obtained from any known load configuration,

T are the surface traction for which K is to be determined,

f are the body forces for which K is to be determined,

Γ is a chosen path around our specimen as to include all the surface tractions T, and

A is the region where the body forces act.

APPENDIX B

JUSTIFICATION OF ASSUMPTIONS

1.   USE OF LINEAR ELASTIC FRACTURE MECHANICS

Linear elastic fracture mechanics (LEFM) requires that the amount of plasticity near the crack tip will be relatively small. As a "rule of thumb" LEFM can be considered to be valid if

$$r_p \leq 0.1a$$

where r_p is the radius of the plastic zone around the crack tip and a is the crack length. Using Irwin's circular model for the plastic zone incorporating the upper bound dimension as obtained by a plane stress solution (Figure B-1),
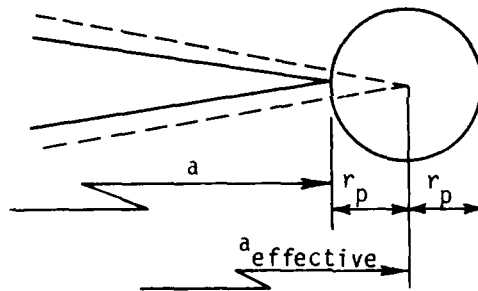
Figure B-1.   Irwin Circular Plastic Zone Model

$$r_p = \frac{1}{2\pi} \left(\frac{K_I}{\sigma_{y \cdot s}} \right)^2 \tag{B-1}$$

where $\sigma_{y \cdot s}$ is the yield strength of the material.
Using 7075 T651

$$\sigma_{y \cdot s} = 80.8 \text{ ksi}$$

The maximum K_I used in our tests was lower than 15 ksi$\sqrt{in}$. Therefore, the maximum radius of plastic zone that has been developed was

$$r_p = \frac{1}{2\pi}\left(\frac{15}{80.8}\right)^2 = 0.0055 \text{ in}$$

The smallest crack length used was

$$a = 0.0815"$$

Thus,

$$\left(\frac{r_p}{a}\right)_{max} = 0.0674 < 0.1$$

The conclusion is that LEFM was valid even in the most extreme conditions. In most cases the crack length was significantly longer and therefore r_p/a smaller.

2. PLANE STRESS/STRAIN CONSIDERATIONS

As a rule of thumb (References 15, 16), if

$$b \geq 2.5\left(\frac{K_{IC}}{\sigma_{y\cdot s}}\right)^2 \tag{B-2}$$

where b is the material thickness, K_{IC} the fracture toughness, and $\sigma_{y\cdot s}$ the yield strength.

The specimen can be considered thick enough to be under a plane strain stress field.

K_{IC} for 7075 T651 plate is 21.4 ksi$\sqrt{in}$.

$$2.5\left(\frac{K_{IC}}{\sigma_{y\cdot s}}\right)^2 = 0.176"$$

Since .24"- .25" thick specimens were used, they can be viewed to be under plane strain conditions.

APPENDIX C

LASER INTERFEROMETER DATA REDUCTION

A typical strip chart recorder trace of fringe motion crack mouth opening and load is shown in Figure C-1. From this chart the fringe order versus load data can be obtained for the left and right fringe pattern as presented in Table C-1. The data can be plotted as shown in Figure C-2.

From Figure C-2 slopes of $\delta m/P$ of the left and right fringe pattern can be obtained by considering only the linear part and ignoring the initial nonlinear part of the plot that is associated with fatigue crack closure effects. Those slopes are averaged to eliminate free body motion.

The experiment is repeated and results are averaged. The value of the slope is used in Equation 33 to get displacement per unit load data. Through Equation 34 stress intensity factors can be calculated.

FULL LOAD SCALE 1000 LB (100 LB/IN)

FULL CRACK MOUTH OPENING (2 η_0)

SCALE 10×10^{-3} IN. $(10^{-3}$ IN/IN)
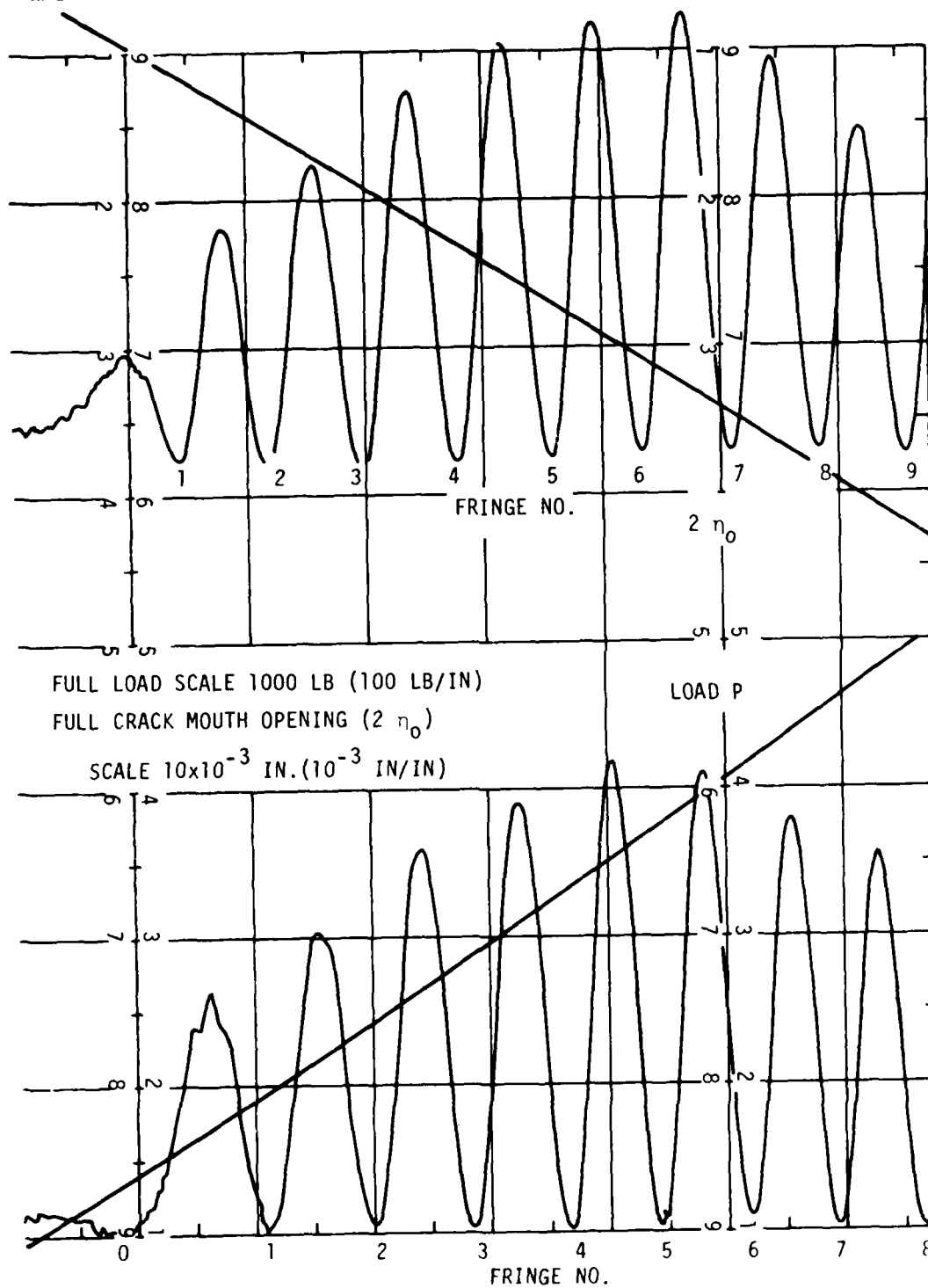
Figure C-1.   Typical Stripchart Recorder Trace of Fringe Motion, Load
and Crack Mouth Opening

TABLE C-1

FRINGE ORDER VERSUS LOAD

Fringe No.	Load Left Pattern	Load Right Pattern
0	120 lb.	60 lb.
1	190 lb.	150 lb.
2	237 lb.	190 lb.
3	278 lb.	235 lb.
4	320 lb.	275 lb.
5	365 lb.	320 lb.
6	410 lb.	360 lb.
7	450 lb.	400 lb.
8	490 lb.	445 lb.
9		485 lb.
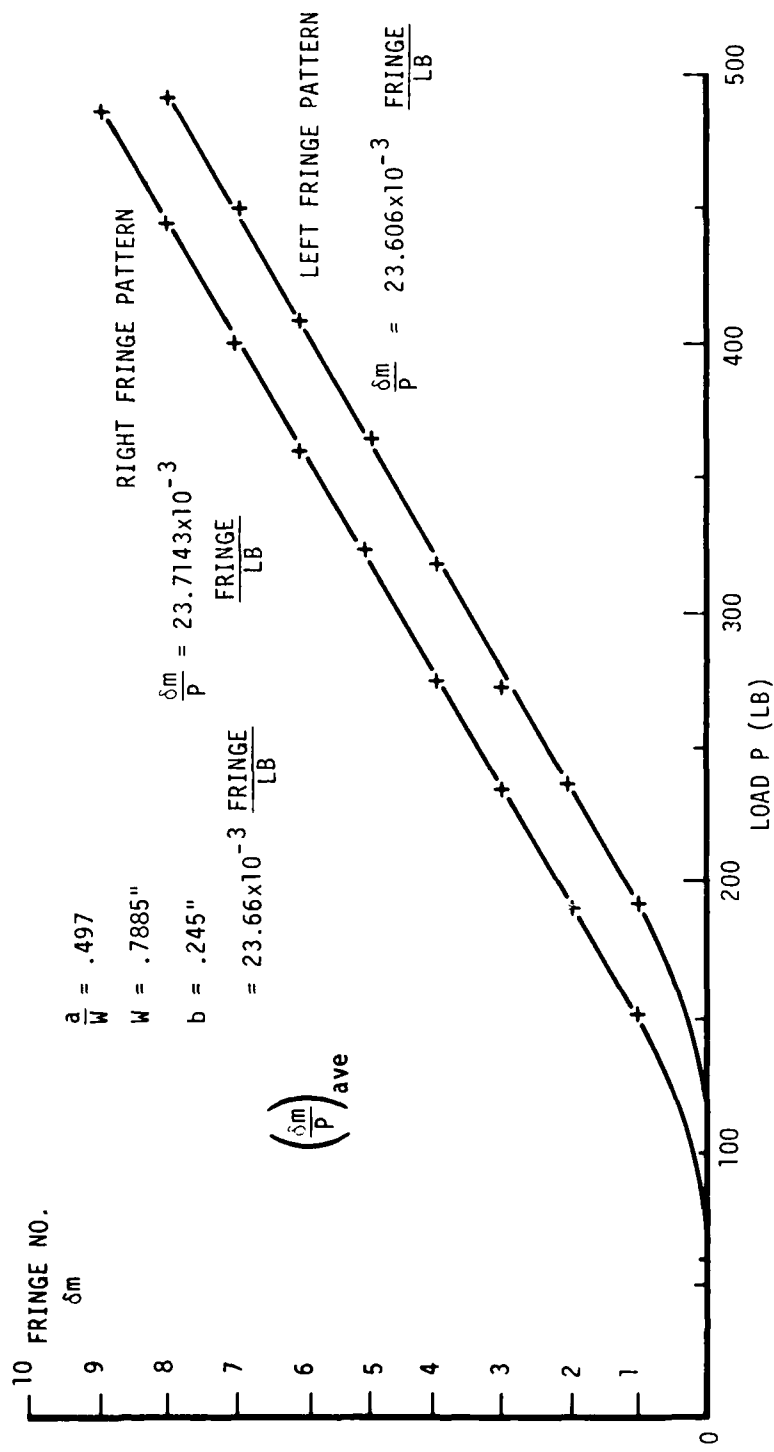
Figure C-2. Typical Load-Fringe Motion Curve

FRINGE NO.
δm

$\dfrac{a}{W} = .497$

$W = .7885''$

$b = .245''$

$= 23.66 \times 10^{-3} \dfrac{\text{FRINGE}}{\text{LB}}$

$\left(\dfrac{\delta m}{P}\right)_{\text{ave}}$

RIGHT FRINGE PATTERN

$\dfrac{\delta m}{P} = 23.7143 \times 10^{-3} \dfrac{\text{FRINGE}}{\text{LB}}$

LEFT FRINGE PATTERN

$\dfrac{\delta m}{P} = 23.606 \times 10^{-3} \dfrac{\text{FRINGE}}{\text{LB}}$

LOAD P (LB)

APPENDIX D

COMPUTER PROGRAM DESCRIPTION

The computer program has been written to perform the numerical computation involved in the process of data interpolation, weight function calculations and finally evaluation of the integral in Equation 30 to determine K_I for Case 2.

In order to allow maximum flexibility in the usage of the program, it was constructed of a main program that performs the integration and nine subprograms that perform all the other necessary calculations. In addition, two library subprograms are used, one from the IMSL library and the other from the CC 6600 library. This structure of the program allows using it for different cases and configurations and permits the user to enter his own interpolation schemes, comparison functions and the noncracked body stress distribution p(t) that makes it possible to compute any desired Case 2 stress intensity factor.

The program is written in FORTRAN and was executed on the CDC system at Wright-Patterson Air Force Base. Execution time for the three-point bending and uniform tension Case 2 stress intensity factor varied from two to four seconds.

1. THE MAIN PROGRAM

The main program reads in the input data, calls in the different subroutines to perform necessary computation and performs the numeric integration by using the IMSL library subprogram DCADRE. An iterative scheme "pushes" down the lower integration limit until the desired accuracy for the end result is met. At the end, it prints out computed K_I for Case 2 compared to user-supplied comparison data.

2. FUNCTION SUBPROGRAM F(x)

This function computes the value of the integrant (the weight function multiplied by P(t)) at each distance t from the crack tip.

3.   FUNCTION SUBPROGRAM P(x)

This function computes the value of the stress at the crack location $P(t)$ for a noncracked body at any distance t from the corresponding crack tip.

The function should be supplied by the user and is the only subprogram that has to be altered when computing K_I for different Case 2 configurations. Care should be taken as related to the form in which $P(t)$ is supplied. This form will determine the form of the calculated K_I. A factor of $1/\sqrt{\pi a}$ is already included in the weight function calculation. So if $P(t)$ is supplied directly in terms of stress, the resulting K_I values will be in the dimensional form of $K_I/\sqrt{\pi a}$.

4.   LIBRARY FUNCTION PLSCF

A CC 6600 Library subroutine, this function computes least square polynomial fits for a given set of data. Polynomials up to 6 degrees or Chebyshev polynomials of any degree can be specified by the user. For further information see Reference 25.

5.   LIBRARY FUNCTION SUBPROGRAM DCADRE

An International Mathematics and Statistics IMSL Library subprogram, this subprogram performs numeric integration of a function using the Romberg extrapolation scheme. The function DCADRE is capable of integrating functions with "jump" discontinuities and certain types of singularity. This feature is most important in our case because of the crack tip singularity of the weight function. Even if the desired accuracy is not found, DCADRE returns the best available estimate. See the IMSL Manual (Reference 26) for further information.

6.   SUBROUTINE KPOL

This subroutine computes a fourth order least square polynomial fit for the nondimensional K_I data using PLSCF subroutine from the CC 6600 library. It prints out the polynomial coefficients C(5)...,C(1) and returns these values to the main program. It also prints out the error flag IER from PLSCF.

7. SUBROUTINE EPOL

This subroutine computes a fourth order least square polynomial fit for the nondimensional η_0 data using PLSCF subroutine from the CC 6600 library. It prints out the polynomial coefficients D(5),...,D(1) and returns them to the main program. It also prints out the error flag IER from PLSCF.

8. SUBROUTINE EVEK

Evaluates the nondimensional K_I from the fourth order least square polynomial and the derivative of K_I with respect to crack length $\partial K_I/\partial a$ at the points where K_I for Case 2 should be evaluated. One should realize that the differentiation considers the fact that the nondimensional K_I usually factors out $1/\sqrt{a}$ that should be included in the differentiated term. The derivative $\partial K_I/\partial a$ requires the expression

$$\frac{\partial K_I}{\partial a} = \frac{\partial (\sigma\sqrt{\pi a}\, Y)}{\partial a} = \sigma\sqrt{\pi a} \left(\frac{Y}{2a} + \frac{\partial Y}{\partial a} \right)$$

where Y is the nondimensional K_I value and σ is the maximum tensile stress in the specimen. K_I and $\partial K_I/\partial a$ are returned to the main program in a dimensional form factored only by $1/\sigma$ as to match the η_0 data.

9. SUBROUTINE EVETTA

Evaluates the nondimensional η_0 from the least square fourth order polynomial and the derivative of η_0 with respect to crack length $\partial \eta_0/\partial a$, at the points where K_I for Case 2 should be evaluated. One should realize that the differentiation considers the fact that the nondimensional η_0 is factored by a term of "a" that should be included in the differentiated term as applied in the above paragraph.

η_0 and $\partial \eta_0/\partial a$ are returned in a dimensional form factored by $1/\sigma$ to match the K_I data.

10. SUBROUTINE COPK

Compares the nondimensional K_I input data with the interpolated data by KPOL at the test points. A comparison table that includes a relative error in percents is printed out for the user's evaluation and judgement.

11. SUBROUTINE COPETA

Compares the nondimensional η_o input data with interpolated data by EPOL at the test points. A comparison table that includes a relative error in percents is printed out for the user's evaluation and judgement.

12. SUBROUTINE KANA

Evaluates K_I for the Case 2 loading configuration from a user-supplied comparison function. The evaluation is done at the same points where K_I Case 2 is evaluated from the experimental data. This subroutine can be eliminated if the above comparison data is available explicitly. In this case, the comparison values should be assigned directly to AK array. If no comparison values are available, the final printout table should be altered to avoid undefined terms.

13. LIST OF SYMBOLS USED IN THE PROGRAM (ALPHABETICAL ORDER)

A	Constant used in subroutine KANA
AERR	Input, absolute error in the integral routine DCADRE
AK(99)	$K_{I_2}/\sigma\sqrt{\pi a}$ comparison value of the K_I Case 2 nondimensional evaluated from the user-supplied comparison function at points defined by S
AKS(99)	$K_{I_2}/\sigma\sqrt{\pi a}$ calculated values of K_I Case 2 (nondimensional) at points defined by S
B	Interim term for weight function calculations
C(5)	Interpolating polynomial coefficients for K_I data
D(5)	Interpolating polynomial coefficients for η_o data
DB	Interim term for weight function calculation
DC	$\partial R/\partial a$ interim term for weight function calculation

DY(99)   Interim derivative term for DYA

DYA(99) $1/\sigma$ $(\partial K_I \partial a)$ derivative w·r·t the crack length of K_I
              Case 1 at points defined by S

D2(99)   Interim derivative term for DZA

DZA(99) $1/\sigma$ $(\partial \eta_0/\partial a)$ derivative w·r·t the crack length of η_0
              at points defined by S

EDS   Input, desired absolute accuracy in K_I computation

ES(99)   (AKS-AK) 100/AK relative error in the computed K_I

EST   Current estimate of value of the integral by DCADRE

EY(99)   (YC-Y) 100/Y relative error in percents of interpolated
              K_I data at points defined by S

EZ(99)   (ZC-Z) 100/Z relative error in percents of interpolated
              η_0 data at points defined by S

F   h, the weight function (subfunction)

G   Upper limit of the integral

H   Input, H material property

IER   Error flag for library subprograms PLSCF and DCADRE

M   Input, number of experimental data points

N   Input, number of points where K_I should be evaluated for
              Case 2

P   Stress distribution for the noncracked body at the crack
              location for Case 2 loading configuration (subfunction)

PI π

Q   Lower limit of integral

R   Interim term for weight function calculation

RELERR   Input, relative error in the integration routine DCADRE

S(99)   Input, a/w, nondimensional crack length at point where
              experiments were performed

T   Interim term for weight function calculations

V   Previous interim value for EST

VA	(EST-V), difference between last and current integration estimate
W(99)	Weight corresponding to each data point used in PLSCF (currently defined as -1 to give equal weight to each point)
WORK(25)	Work array for PLSCF subroutine
X(99)	Input, a/w, nondimensional crack length for points where K_I Case 2 should be evaluated
Y(99)	Input, $K_I / \sigma\sqrt{\pi a}$, nondimensional K_I, experimental data
YA(99)	KI/σ, interpolated K_I for Case 1 at points defined by x
YC(99)	$K_I / \sigma\sqrt{\pi a}$, interpolated nondimensional K_I for Case 1 at points defined by S
YK(99)	$K_I / \sigma\sqrt{\pi a}$, interpolated nondimensional K_I for Case 1 at points defined by x
Z(99)	Input, $\eta_0 \cdot H/(2\sigma a)$, nondimensional crack mouth opening
ZA(99)	η_0/σ, interpolated η_0 at the points defined by x
ZC(99)	$\eta_0 H/(2\sigma a)$, interpolated nondimensional η_0 at points defined by S
ZK(99)	$\eta_0 H/(2\sigma a)$, interpolated nondimensional η_0 at points defined by x

14. SEQUENCE OF INPUT DATA

Card Number	Variable	No. of Variables per card	Real/ Integer	Format
1	H	1	Real	Unformatted
2	AERR,RELERR,EPS	3	Real	Unformatted
3	M	1	Integer	Unformatted
3 to (M+3)	S(I),Y(I),Z(I)	3	Real	Unformatted
M+4	N	1	Integer	Unformatted
(M+5) to (M+N+5)	X(I)	1	Real	Unformatted

63

15. SEQUENCE OF OUTPUT DATA

    1.   Interpolation polynomial coefficients for K_I

    2.   Interpolation polynomial coefficients for η_o

    3.   Comparison table of actual to interpolated K_I

    4.   Comparison table of actual to interpolated η_o

    5.   The following printout will appear only if singularities have been met by subroutine DCADRE. Each time a singularity was met, a warning statement is printed out followed by the values of the crack length (X(I)), the distance from crack tip (Q), and the value of the error flag (IER) for which the singularity occurred. Values of IER equal to 65 or 66 indicate that the singularity was successfully handled. If any other value appears consult the IMSL Manual (Reference 26).

    6.   Comparison table of K_I for Case 2 calculated values and supplied comparison values.

16. LISTING AND RESULT SAMPLE

    The following pages include a complete listing of the program and a sample printout of results for uniform tension as Case 2 loading configuration.

```
1              PROGRAM TH 5 (INPUT=/80,OUTPUT)
        C
        C**************************  DECEMBER 1979  **********************************
        C    DATA REDUCTION FOR THSIS -DAN BAR-TIKVA
5       C    (SEE THSIS APPENDIX (AFIT/GAE/AA/79D-2 ) FOR DETAILED DESCRIPTION)
        C
        C
               DIMENSION X(99),Y(99),Z(99),S(99),YK(99),YA(99),YC(99),DYA(99),DY(
              099),EY(99),ZK(99),ZA(99),ZC(99),)ZA(99),DZ(99),AK(99),AKS(99),ES(9
10            099),C(5),D(5),WORK(29),W(99),EZ(99)
               COMMON/DAN/G,T,B,R,DB,DC
               EXTERNAL F
               PI=4.*ATAN(1.8)
        C    FIRST CARD
15      C    READ IN M
               READ*,M
        C    SECCOND CARD
        C    READ IN THE FOLLOING TERMS ON THE SAME CARD(UNFORMATTED)
        C    AERR-ABSOLUT ERROR IN THE INTEGRAL ROUTINE(DCADRE)
20      C    RELERR-RELATIVE ERROR IN THE INTEGRATION ROUTINE(DCADRE)
        C    EPS-DESIRED ABSOLUTE ACCURACY IN ANSWER
               READ* ,AERR,RELERR,EPS
        C    NEXT CARD-NUMBER OF EXPERIMENTAL DATA POINTS
               READ* ,M
25      C    THE NEXT M CARDS CONTAINE THE EXPERIMENTAL DATA THREE VALUES ON EACH
        C    CARD-A/M,K(NON DIMENSIONAL),ETA(NON DIMENSIONAL)-  (UNFORMATTED)
               DO 2 I=1,M
2              READ* ,S(I),Y(I),Z(I)
        C    NEXT CARD-N-NUMBER OF POINTS WHERE K SHOULD BE EVALUATED FOR CASE 2
30             READ* ,N
        C    NEXT N CARDS-VALUES OF A/W AT WHICH K SHOULD BE EVALUATED (ONE VALUE PER
        C    CARD-UNFORMATTED)
               DO 17 I=1,N
17             READ* ,X(I)
35             PRINT 1
1              FORMAT(1H1,18X,"RESULTS")
               PRINT*," "           *******"
               PRINT*," "
               PRINT*," "
40             PRINT*," "
               PRINT*," "
        C    COMPUTE A LEAST SQUARE FORTH ORDER POLYNOMIAL FOR K  DATA AND PRINT OUT
        C    POLYNOMIAL COEFFITIENTS C(5)....C(1) AND ERROR FLAG OF  SUBROUTINE PLSCF
               CALL KPOL(S,Y,M,C,WORK,M)
45      C    COMPUTE A LEAST SQUARE FORTH ORDER POLYNOMIAL FOR ETA DATA AND PRINT OUT
        C    POLYNOMIAL COEFFITIENTS D(5)....D(1) AND ERROR FLAG OF  SUBROUTINE PLSCF
               CALL EPOL(S,Z,M,D,WORK,M)
        C    EVALUATE  K  AND ITS DERIVATIVES FROM THE LEAST SQUARE POLYNOMIAL
               CALL EVEK(X,C,PI,N,YK,DYA,YA,DY)
50      C    EVALUATE ETA AND ITS DERIVATIVES FROM THE LEAST SQUARE POLYNOMIAL
               CALL EVEETA(X,D,M,N,ZK,DZA,ZA,DZ)
        C    COMPARE THE ACTUAL EXPERIMENTAL K  DATA WITH THE LEAST SQUARE FIT
               CALL COPK(S,Y,C,M,YC,EY)
        C    COMPARE THE ACTUAL EXPERIMENTAL ETA DATA WITH THE LEAST SQUARE FIT
55             CALL COPETA(S,Z,D,M,ZC,EZ)
        C    COMPUTE COMPARISON VALUES FOR  K  CASE 2 (USER SUPPLIED ROUTINE)
               CALL KANA(X,N,AK,PI)
```

```
                PRINT*," "
                PRINT*," "
60              PRINT*," "
                PRINT*," "
        C   COMPUTE K FOR CASE 2 AND PRINT OUT A COMPARISON TABLE BETWEEN THE CALCULATED
        C   VALUES AND THE SUPPLIED COMPARISON VALUES
        C
65              PRINT*,"THE FOLLOING PRINT OUT IS FROM THE NUMERICAL INTEGRATION"
                PRINT*,"SUBROUTINE(DCADRE) AND INDICATS THAT SINGULARITIES WHERE"
                PRINT*,"HANDLED"
                PRINT*," "
                PRINT*,"   IER=ERROR FLAG,IF 65 OR 66 -SINGULARITIES WHERE SUCCESS
               *FULLY HANDLED,ANY ATHFP VALUE CONSULT IMSL MANUAL"
70              PRINT*,"   X(I)=THE CRACK LENGTH  FOR WHICH THE ERROR FLAG(IER) IM
               *PLIES"
                PRINT*,"   Q=DISTANCE FROM CRACK TIP RELATIVE TO WIDTH   (T/W) FOR
               *WHICH THE SINGULARITY WAS DETACTED"
75              PRINT*," "
                PRINT*," "
                PRINT*," "
                DO 6 I=1,N
                PRINT*," "
80              PRINT*," "
                B=8.*(YA(I))**2/(PI*H**2)
                DB=16.*YA(I)*DYA(I)/(PI*H**2)
                R=(ZA(I)/X(I))**2-8.*(YA(I))**2/(PI*X(I)*H**2)
                DC=-2.*(ZA(I))**2/(X(I))**3-16.*YA(I)/(PI*X(I)*H**2)*DYA(I)+8.*(YA
               *(I))**2/(PI*(H*X(I))**2)+2.*ZA(I)*DZA(I)/(X(I))**2
85              G=X(I)
                T=H/(((PI*X(I))**.5)*YA(I))
                V=0.
                Q=.000001
90         15   Q=Q*.1
                EST=     DCADRF(F,Q,G,AERR,RELERR,ERROR,IER)
                IF(IER.EQ.0) GO TO 21
                PRINT*,"X(",I,")=",X(I)
                PRINT*,"Q=",Q
95              PRINT*,"IER=",IER
           21   CONTINUE
                VA=EST-V
                IF(VA.LE.EPS)   GO TO 16
                V=EST
100             GO TO 15
           16   CONTINUE
                AKS(I)=EST
                ES(I)=(AKS(I)-AK(I))*100./AK(I)
            6   CONTINUE
105             PRINT*," "
                PRINT*," "
                PRINT*," "
                PRINT*," "
                PRINT*," "
110             PRINT*," "
                PRINT*," "
                PRINT*,"  RESULTS FOR  K  UNIFORM TENSION USING THE WEIGHT FUNCTIO
               *N METHOD(K-NON DIMENSIONAL"
                PRINT*,"---------------------------------------------------------"
```

```
  PROGRAM TH5        74/74    OPT=1                    FTN 4.7+476      09/28/79  18.07.02      PAGE    3

115              C----------------------------"
                 PRINT*," "
                 PRINT*," "
                 PRINT*,"   A/W - CRACK LENGTH RELATIVE TO WIDTH "
                 PRINT*,"   K-EXP - VALUES CALCULATED THROUGH THE WEIGH FUNCTION"
120              PRINT*,"   K-CAL - SUPPLIED COMPERISON VALUES"
                 PRINT*,"   E     - RELATIVE ERROR IN X"
                 PRINT*," "
                 PRINT*," "
                 PRINT*,"   A/W       K-EXP     K-CAL        E"
125              PRINT*," "
                 DO 13 I=1,N
                 PRINT 10,X(I),AKS(I),AK(I),ES(I)
        10       FORMAT(1X,1F6.4,4X,1F8.4,2X,1F8.4,2X,1F6.2)
        13       CONTINUE
130              STOP"END OF PROGRAM"
                 END




  FUNCTION F         74/74    OPT=1                    FTN 4.7+476      09/28/79  18.07.02      PAGE    1

1                FUNCTION F(X)
                 EXTERNAL P
                 COMMON/DAN/G,T,B,R,DB,DC
                 F=(T/2.)*(B+DB*X+DC*X**2+2.*R*X)/((B*X+R*X**2)**.5)*P(X)
9                RETURN
                 END




  FUNCTION P         74/74    OPT=1                    FTN 4.7+476      09/28/79  18.07.02      PAGE    1

1                FUNCTION P(X)
                 COMMON/DAN/G,T,B,R,DB,DC
                 P=1.
                 RETURN
9                END
```

```
SUBROUTINE KPOL        74/74    OPT=1                    FTN 4.7+476      09/28/79  18.07.02      PAGE    1

1               SUBROUTINE KPOL(X,Y,M,C,WORK,W)
                DIMENSION X(1),Y(1),C(F),WORK(1),W(1)
                NDEG=4
                NP=M
5               W(1)=-1.
                IN=0
                CALL PLSCF(X,Y,W,NP,NDEG,NMAX,C,IN,XD,X0,WORK,IER)
                PRINT*," "
                PRINT*," "
10              PRINT*,"        INTERPOLATION POLINOMIAL FOR K     "
                PRINT*," "
                PRINT*," "
                PRINT*,"C(5)=",C(5)
                PRINT*,"C(4)=",C(4)
15              PRINT*,"C(3)=",C(3)
                PRINT*,"C(2)=",C(2)
                PRINT*,"C(1)=",C(1)
                PRINT*," "
                PRINT*,"IER- ERROR FLAG-SEE ASD COMPUTER SUBPROGRAM LIBRARY GUIDE"
20              PRINT*,"IER=",IER
                RETURN
                END

SUBROUTINE EPOL        74/74    OPT=1                    FTN 4.7+476      09/28/79  18.07.02      PAGE    1

1               SUBROUTINE EPOL(X,Z,M,D,WORK,W)
                DIMENSION X(1),Z(1),D(5),WORK(1),W(1)
                NDEG=4
                NP=M
5               IN=0
                W(1)=-1.
                CALL PLSCF(X,Z,W,NP,NDEG,NMAX,D,IN,XD,X0,WORK,IER)
                PRINT*," "
                PRINT*," "
10              PRINT*,"        INTERPOLATION POLINOMIAL FOR ETA   "
                PRINT*," "
                PRINT*,"D(5)=",D(5)
                PRINT*,"D(4)=",D(4)
                PRINT*,"D(3)=",D(3)
15              PRINT*,"D(2)=",D(2)
                PRINT*,"D(1)=",D(1)
                PRINT*," "
                PRINT*,"IER- ERROR FLAG-SEE ASD COMPUTER SUBPROGRAM LIBRARY GUIDE"
                PRINT*,"IER=",IER
20              RETURN
                END

SUBROUTINE EVEK        74/74    OPT=1                    FTN 4.7+476      09/28/79  18.07.02      PAGE    1

1               SUBROUTINE EVEK(X,C,PI,N,YK,DYA,YA,DY)
                DIMENSION X(1),C(5),YK(1),DYA(1),YA(1),DY(1)
                DO 1 I=1,N
                YK(I)=C(5)*X(I)**4+C(4)*X(I)**3+C(3)*X(I)**2+C(2)*X(I)+C(1)
5               YA(I)=YK(I)*(X(I)*PI)**.5
                DY(I)=4*C(5)*X(I)**3+3*C(4)*X(I)**2+2.*C(3)*X(I)+C(2)
1               DYA(I)=(PI**.5)*(YK(I)/(2.*X(I))+DY(I))*X(I)**0.5
                RETURN
                END
```

```
SUBROUTINE COPK      74/74    OPT=1                    FTN 4.7+476      09/26/79  18.07.02      PAGE    1

   1              SUBROUTINE COPK(X,Y,C,M,YC,EY)
                  DIMENSION X(1),Y(1),C(5),YC(1),EY(1)
                  DO 18 I=1,M
                  YC(I)=C(5)*X(I)**4+C(4)*X(I)**3+C(3)*X(I)**2+C(2)*X(I)+C(1)
   5        18    EY(I)=(YC(I)-Y(I))*100./Y(I)
                  PRINT*," "
                  PRINT*," "
                  PRINT*," "
                  PRINT*," "
  18              PRINT*,"COMPERISON OF ACTUAL DATA TO INTERPOLATED DATA"
                  PRINT*," "
                  PRINT*,"    A/W - CRACK LENGTH RELATIVE TO WIDTH "
                  PRINT*,"     K-EXP   ACTUAL DATA"
                  PRINT*,"     K-CAL   INTERPOLATED DATA"
  15              PRINT*,"     E       RELATIVE ERROR IN X"
                  PRINT*," "
                  PRINT*," "
                  PRINT*,"    A/W    K-EXP     K-CAL      E "
                  PRINT*," "
  20              DO 4 I=1,M
                  PRINT 3,X(I),Y(I),YC(I),EY(I)
        3         FORMAT(1X,1F6.4,4X,1F8.4,2X,1F8.4,2X,1F6.2)
        4         CONTINUE
                  RETURN
  25              END
```

```
SUBROUTINE COPETA    74/74    OPT=1                    FTN 4.7+476      09/26/79  18.07.02      PAGE    1

   1              SUBROUTINE COPETA(X,Z,D,M,ZC,EZ)
                  DIMENSION X(1),Z(1),D(5),ZC(1),EZ(1)
                  DO 19 I=1,M
                  ZC(I)=D(5)*X(I)**4+D(4)*X(I)**3+D(3)*X(I)**2+D(2)*X(I)+D(1)
   5        19    EZ(I)=(ZC(I)-Z(I))*100./Z(I)
                  PRINT*," "
                  PRINT*," "
                  PRINT*," "
                  PRINT*," "
  18              PRINT*,"COMPERISON OF ACTUAL DATA TO INTERPOLATED DATA"
                  PRINT*," "
                  PRINT*,"    A/W - CRACK LENGTH RELATIVE TO WIDTH "
                  PRINT*,"    ETA-EXP   ACTUAL DATA"
                  PRINT*,"    ETA-CAL   INTERPOLATED DATA"
  15              PRINT*,"     E       RELATIVE ERROR IN X"
                  PRINT*," "
                  PRINT*," "
                  PRINT*," "
                  PRINT*,"    A/W    ETA-EXP   ETA-CAL      E      "
  20              PRINT*," "
                  DO 7 I=1,M
                  PRINT 9,X(I),Z(I),ZC(I),EZ(I)
        9         FORMAT(1X,1F6.4,4X,1F8.4,2X,1F8.4,2X,1F6.2)
        7         CONTINUE
  25              RETURN
                  END
```

69

```
SUBROUTINE EVEETA      74/74   OPT=1                    FTN 4.7+476      09/28/79  10.07.02      PAGE    1

1               SUBROUTINE EVEETA(X,D,H,N,ZK,DZA,ZA,DZ)
                DIMENSION X(1),D(5),ZK(1),DZA(1),ZA(1),DZ(1)
                DO 5 I=1,N
                ZK(I)=D(5)*X(I)**4+D(4)*X(I)**3+)(3)*X(I)**2+D(2)*X(I)+D(1)
5               ZA(I)=ZK(I)*2.*X(I)/H
                DZ(I)=4*D(5)*X(I)**3+3*D(4)*X(I)**2+2.*D(3)*X(I)+D(2)
        5       DZA(I)= (2./H)*(DZ(I)*Y(I)+ZK(I))
                RETURN
                END


SUBROUTINE KANA        74/74   OPT=1                    FTN 4.7+476      09/28/79  10.07.02      PAGE    1

1               SUBROUTINE KANA(X,N,AK,PI)
                DIMENSION X(1),AK(1)
                DO 20 I=1,N
                A=X(I)*PI/2.
5               AK(I)=((2.*TAN(A)/(PI*X(I))) **.5)*((.752+2.02*X(I)+.37*(1.-SIN(A)
               8)**3.)/COS(A))
        20      CONTINUE
                RETURN
                END
```

RESULTS

INTERPOLATION POLINOMIAL FOR K

C(5)=78.75542913721
C(4)=-92.45527346502
C(3)=42.95455968156
C(2)=-6.528725084317
C(1)=1.256607805434

IER- ERROR FLAG-SEE ASD COMPUTER SUBPROGRAM LIBRARY GUIDE
IER=0

INTERPOLATION POLINOMIAL FOR ETA

D(5)=210.3785059491
D(4)=-282.572732332
D(3)=150.7543048959
D(2)=-32.16174824838
D(1)=3.952885733928

IER- ERROR FLAG-SEE ASD COMPUTER SUBPROGRAM LIBRARY GUIDE
IER=0

COMPERISON OF ACTUAL DATA TO INTERPOLATED DATA

A/W - CRACK LENGTH RELATIVE TO WIDTH
K-EXP   ACTUAL DATA
K-CAL   INTERPOLATED DATA
E   RELATIVE ERROR IN X

A/W	K-EXP	K-CAL	E
.1034	.9073	.9467	4.34
.1586	1.0575	.9776	-7.56
.2004	1.0572	1.0545	-.26
.2328	1.1137	1.1060	-.69
.2646	1.1007	1.1705	6.35
.2666	1.1862	1.1746	-.98
.3096	1.2366	1.2590	1.81
.3468	1.3490	1.3244	-1.82
.3978	1.3804	1.4086	2.04
.4360	1.4388	1.4696	2.14
.4760	1.5646	1.5424	-1.42
.4893	1.6551	1.5710	-5.08
.5788	1.8481	1.8774	1.59
.6467	2.3468	2.3688	.97
.7517	3.9513	3.9413	-.25

COMPERISON OF ACTUAL DATA TO INTERPOLATED DATA

```
   A/W - CRACK LENGTH RELATIVE TO WIDTH
  ETA-EXP   ACTUAL DATA
  ETA-CAL   INTERPOLATED DATA
    E       RELATIVE ERROR IN %
```

A/W	ETA-EXP	ETA-CAL	E
.1034	1.9440	1.9508	.31
.1586	1.6643	1.6491	-.91
.2064	1.6855	1.6334	-3.09
.2328	1.6163	1.6879	4.43
.2646	1.6958	1.7933	5.88
.2666	1.8796	1.8011	-4.18
.3096	1.9961	1.9923	-.19
.3460	2.1660	2.1823	.75
.3978	2.6055	2.4945	-4.26
.4360	2.7493	2.7696	.74
.4768	3.0632	3.1251	2.02
.4893	3.2866	3.2648	-.66
.5780	4.5933	4.6431	1.08
.6467	5.6244	6.5725	-.78
.7517	12.0988	12.1882	.08

THE FOLLOING PRINT OUT IS FROM THE NUMERICAL INTEGRATION
SUBROUTINE(DCADRE) AND INDICATS THAT SINGULARITIES WHERE
HANDLED

```
   IER=ERROR FLAG,IF 65 OR 66 -SINGULARITIES WHFRE SUCCESSFULLY HANDLED,ANY ATHER VALUE CONSULT IMSL MANUAL
   X(I)=THE CRACK LENGTH  FOR WHICH THE ERROR FLAG(IER) IMPLIES
   Q=DISTANCE FROM CRACK TIP RELATIVE TO WIDTH  (T/W) FOR WHICH THE SINGULARITY WAS DETACTED
```

```
*** WARNING WITH FIX ERROR  (IER = 65) FROM IMSL ROUTINE DCADRE
X(1)=.1
Q=1.E-11
IER=65
*** WARNING WITH FIX ERROR  (IER = 65) FROM IMSL ROUTINE DCADRE
X(1)=.1
Q=1.E-12
IER=65

*** WARNING WITH FIX ERROR  (IER = 65) FROM IMSL ROUTINE DCADRE
X(2)=.15
Q=1.E-10
IER=65
*** WARNING WITH FIX ERROR  (IER = 65) FROM IMSL ROUTINE DCADRE
X(2)=.15
Q=1.E-11
IER=65
*** WARNING WITH FIX ERROR  (IER = 65) FROM IMSL ROUTINE DCADRE
X(2)=.15
Q=1.E-12
IER=65
```

```
*** WARNING WITH FIX ERROR  (IER =  65) FROM IMSL ROUTINE DCADRE
X(3)=.2
Q=1.E-10
IER=65
*** WARNING WITH FIX ERROR  (IER =  65) FROM IMSL ROUTINE DCADRE
X(3)=.2
Q=1.E-11
IER=65
*** WARNING WITH FIX ERROR  (IER =  65) FROM IMSL ROUTINE DCADRE
X(3)=.2
Q=1.E-12
IER=65


*** WARNING WITH FIX ERROR  (IER =  65) FROM IMSL ROUTINE DCADRE
X(4)=.25
Q=1.E-10
IER=65
*** WARNING WITH FIX ERROR  (IER =  65) FROM IMSL ROUTINE DCADRE
X(4)=.25
Q=1.E-11
IER=65
*** WARNING WITH FIX ERROR  (IER =  65) FROM IMSL ROUTINE DCADRE
X(4)=.25
Q=1.E-12
IER=65


*** WARNING WITH FIX ERROR  (IER =  65) FROM IMSL ROUTINE DCADRE
X(5)=.3
Q=1.E-9
IER=65
*** WARNING WITH FIX ERROR  (IER =  65) FROM IMSL ROUTINE DCADRE
X(5)=.3
Q=1.E-10
IER=65
*** WARNING WITH FIX ERROR  (IER =  65) FROM IMSL ROUTINE DCADRE
X(5)=.3
Q=1.E-11
IER=65
*** WARNING WITH FIX ERROR  (IER =  65) FROM IMSL ROUTINE DCADRE
X(5)=.3
Q=1.E-12
IER=65


*** WARNING WITH FIX ERROR  (IER =  65) FROM IMSL ROUTINE DCADRE
X(6)=.35
Q=1.E-9
IER=65
*** WARNING WITH FIX ERROR  (IER =  65) FROM IMSL ROUTINE DCADRE
X(6)=.35
Q=1.E-10
IER=65
*** WARNING WITH FIX ERROR  (IER =  65) FROM IMSL ROUTINE DCADRE
X(6)=.35
Q=1.E-11
IER=65
*** WARNING WITH FIX ERROR  (IER =  65) FROM IMSL ROUTINE DCADRE
X(6)=.35
Q=1.E-12
IER=65
```

```
*** WARNING WITH FIX ERROR  (IER =  65) FROM IMSL ROUTINE DCADRE
X(7)=.4
Q=1.E-9
IER=65
*** WARNING WITH FIX ERROR  (IER =  65) FROM IMSL ROUTINE DCADRE
X(7)=.4
Q=1.E-10
IER=65
*** WARNING WITH FIX ERROR  (IER =  65) FROM IMSL ROUTINE DCADRE
X(7)=.4
Q=1.E-11
IER=65
*** WARNING WITH FIX ERROR  (IER =  65) FROM IMSL ROUTINE DCADRE
X(7)=.4
Q=1.E-12
IER=65


*** WARNING WITH FIX ERROR  (IER =  65) FROM IMSL ROUTINE DCADRE
X(8)=.45
Q=1.E-9
IER=65
*** WARNING WITH FIX ERROR  (IER =  65) FROM IMSL ROUTINE DCADRE
X(8)=.45
Q=1.E-10
IER=65
*** WARNING WITH FIX ERROR  (IER =  65) FROM IMSL ROUTINE DCADRE
X(8)=.45
Q=1.E-11
IER=65


*** WARNING WITH FIX ERROR  (IER =  65) FROM IMSL ROUTINE DCADRE
X(9)=.5
Q=1.E-9
IER=65
*** WARNING WITH FIX ERROR  (IER =  65) FROM IMSL ROUTINE DCADRE
X(9)=.5
Q=1.E-10
IER=65
*** WARNING WITH FIX ERROR  (IER =  65) FROM IMSL ROUTINE DCADRE
X(9)=.5
Q=1.E-11
IER=65


*** WARNING WITH FIX ERROR  (IER =  65) FROM IMSL ROUTINE DCADRE
X(10)=.55
Q=1.E-9
IER=65
*** WARNING WITH FIX ERROR  (IER =  65) FROM IMSL ROUTINE DCADRE
X(10)=.55
Q=1.E-10
IER=65
*** WARNING WITH FIX ERROR  (IER =  65) FROM IMSL ROUTINE DCADRE
X(10)=.55
Q=1.E-11
IER=65


*** WARNING WITH FIX ERROR  (IER =  65) FROM IMSL ROUTINE DCADRE
X(11)=.6
Q=1.E-9
IER=65
*** WARNING WITH FIX ERROR  (IER =  65) FROM IMSL ROUTINE DCADRE
X(11)=.6
```

```
. ... ..
IER=65
*** WARNING WITH FIX ERROR  (IER =  65) FROM IMSL ROUTINE DCADRE
X(11)=.6
Q=1.E-11
IER=65


*** WARNING WITH FIX ERROR  (IER =  65) FROM IMSL ROUTINE DCADRE
X(12)=.65
Q=1.E-8
IER=65
*** WARNING WITH FIX ERROR  (IER =  65) FROM IMSL ROUTINE DCADRE
X(12)=.65
Q=1.E-9
IER=65
*** WARNING WITH FIX ERROR  (IER =  65) FROM IMSL ROUTINE DCADRE
X(12)=.65
Q=1.E-10
IER=65
*** WARNING WITH FIX ERROR  (IER =  65) FROM IMSL ROUTINE DCADRE
X(12)=.65
Q=1.E-11
IER=65


*** WARNING WITH FIX ERROR  (IER =  66) FROM IMSL ROUTINE DCADRE
X(13)=.7
Q=1.E-7
IER=66
*** WARNING WITH FIX ERROR  (IER =  66) FROM IMSL ROUTINE DCADRE
X(13)=.7
Q=1.E-8
IER=66
*** WARNING WITH FIX ERROR  (IER =  66) FROM IMSL ROUTINE DCADRE
X(13)=.7
Q=1.E-9
IER=66
*** WARNING WITH FIX ERROR  (IER =  66) FROM IMSL ROUTINE DCADRE
X(13)=.7
Q=1.E-10
IER=66
*** WARNING WITH FIX ERROR  (IER =  66) FROM IMSL ROUTINE DCADRE
X(13)=.7
Q=1.E-11
IER=66


*** WARNING WITH FIX ERROR  (IER =  65) FROM IMSL ROUTINE DCADRE
X(14)=.75
Q=1.E-8
IER=65
*** WARNING WITH FIX ERROR  (IER =  65) FROM IMSL ROUTINE DCADRE
X(14)=.75
Q=1.E-9
IER=65
*** WARNING WITH FIX ERROR  (IER =  65) FROM IMSL ROUTINE DCADRE
X(14)=.75
Q=1.E-10
IER=65
*** WARNING WITH FIX ERROR  (IER =  65) FROM IMSL ROUTINE DCADRE
X(14)=.75
Q=1.E-11
IER=65
```

```
... WARNING WITH FIX ERROR    (IER =  66) FROM IMSL ROUTINE DCADRE
X(15)=.8
Q=1.E-7
IER=66
*** WARNING WITH FIX ERROR   (IER =  66) FROM IMSL ROUTINE DCADRE
X(15)=.8
Q=1.E-8
IER=66
*** WARNING WITH FIX ERROR   (IER =  66) FROM IMSL ROUTINE DCADRE
X(15)=.8
Q=1.E-9
IER=66
*** WARNING WITH FIX ERROR   (IER =  66) FROM IMSL ROUTINE DCADRE
X(15)=.8
Q=1.E-10
IER=66
*** WARNING WITH FIX ERROR   (IER =  66) FROM IMSL ROUTINE DCADRE
X(15)=.8
Q=1.E-11
IER=66
```

RESULTS FOR K UNIFORM TENSION USING THE WEIGHT FUNCTION METHOD(K-NON DIMENSIONAL

```
    A/W - CRACK LENGTH RELATIVE TO WIDTH
    K-EXP - VALUES CALCULATED THROUGH THE WEIGH FUNCTION
    K-CAL - SUPPLIED COMPERISON VALUES
    E     - RELATIVE ERROR IN %

    A/W      K-EXP     K-CAL       E

    .1000    1.2705    1.1957      6.26
    .1500    1.2697    1.2682       .12
    .2000    1.4041    1.3667      2.74
    .2500    1.5548    1.4941      4.01
    .3000    1.6855    1.6551      1.83
    .3500    1.8170    1.8565     -2.13
    .4000    1.9967    2.1080     -5.28
    .4500    2.2917    2.4241     -5.46
    .5000    2.7719    2.8266     -1.93
    .5500    3.4752    3.3486      3.78
    .6000    4.3636    4.0432      7.92
    .6500    5.3158    4.9993      6.33
    .7000    6.1832    6.3755     -3.02
    .7500    6.8662    8.4809    -19.04
    .8000    7.3408   11.9926    -38.79
```

APPENDIX E

CRACK SHAPE--CONICAL APPROXIMATION

Following Orange (Reference 11), the shape of a crack can be
approximated by a conic section equation. Requiring that the crack
opening at the crack mouth will match the actual crack mouth opening
η_o, one can write a general form for the conic section; equation;

$$\left(\frac{\eta}{\eta_o}\right)^2 = \frac{2}{(2+\bar{m})}\left(\frac{t}{a}\right) + \frac{\bar{m}}{2+\bar{m}}\left(\frac{t}{a}\right)^2 \tag{E-1}$$
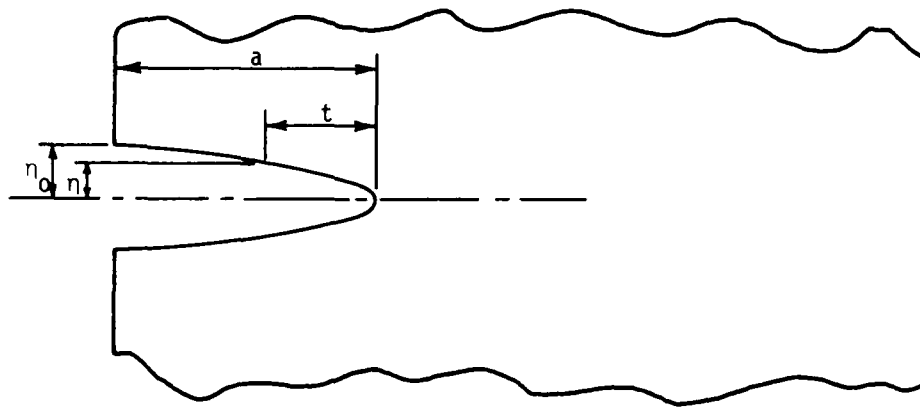

Figure E-1. Crack Opening Conical Approximation

where t is the distance from the crack tip, a is the crack length, and $\bar{m}$
is the conic section coefficient to be determined. The type of conical
section depends on $\bar{m}$ if

$\bar{m} < 0$ – ellipse

$\bar{m} = 0$ – parabola

$0 < \bar{m} < \infty$ – hyperbola

$\bar{m} = \infty$ – a pair of straight lines

In order to determine the unknown conic section coefficient $\bar{m}$, match the radius of curvature at the crack tip from the Equation E-1 to the curvature resulting from the crack tip displacement field as expressed in Equation 16.

Using the following definition for the curvature of a two-dimensional curve defined by

$$y = f(x) \tag{E-2}$$

the curvature $\bar{K}$ is given by

$$K = \frac{-\dfrac{d^2x}{dy^2}}{\left\{ 1 + \left(\dfrac{dx}{dy}\right)^2 \right\}^{\frac{3}{2}}} \tag{E-3}$$

and the radius of curvature is

$$\bar{R} = \left[\frac{1}{\bar{K}} \right] \tag{E-4}$$

provided $\bar{K} \neq 0$

If one uses the near crack tip displacement field from Equation 16,

$$t = \frac{\pi H^2}{8K_I} \, \eta^2 \tag{E-5}$$

$$\frac{\partial t}{\partial \eta} = \frac{\pi H^2}{4K_I} \, \eta \tag{E-6}$$

and at the crack tip

$$\eta = 0$$

$$t = 0.$$

From Equation E-6

$$\left.\frac{\partial t}{\partial \eta}\right|_{\eta=0} = 0 \qquad (E-7)$$

Also from Equation E-6

$$\frac{\partial^2 t}{\partial \eta^2} = \frac{\pi H^2}{4K_I} \qquad (E-8)$$

Substituting Equations E-7, E-8 into Equation E-3 and then using Equation E-4, the radius of curvature at the crack tip from the crack tip displacement field is

$$\bar{R} = \frac{4K_I^2}{\pi H^2} \qquad (E-9)$$

Now find the radius of curvature from the conic section Equation E-1

$$\eta^2 = \frac{2\eta_o^2}{(2+\bar{m})a} \, t \; + \; \frac{\bar{m}\eta_o^2}{(2+\bar{m})a^2} \, t^2 \qquad (E-10)$$

Differentiate twice with respect to η

$$2\eta = \frac{2\eta_o}{(2+\bar{m})a} \; \frac{\partial t}{\partial \eta} + \frac{2\bar{m}\eta_o^2}{(2+\bar{m})a^2} \; t \cdot \frac{\partial t}{\partial \eta} \qquad (E-11)$$

$$2 = \frac{2\eta_o^2}{(2+\bar{m})a} \; \frac{\partial^2 t}{\partial \eta^2} + \frac{2\bar{m}\eta_o^2}{(2+\bar{m})a^2} \left[\left(\frac{\partial t}{\partial \eta}\right)^2 + t \; \frac{\partial^2 t}{\partial \eta^2} \right] \qquad (E-12)$$

From Equations E-11 and E-12 at the crack tip

$$t=0, \quad \eta=0$$

The value

$$\frac{\partial t}{\partial \eta} = 0$$

and

$$\frac{\partial^2 t}{\partial \eta^2} = \frac{(2+\bar{m})a}{\eta_o^2} \qquad \text{(E-13)}$$

If Equations E-3 and E-4 are used, the radius of curvature at the tip of the conic section is

$$R = \frac{\eta_o^2}{(\bar{m}+2)a} \qquad \text{(E-14)}$$

Now, matching the radius of curvature at the crack tip of the conic section (Equation E-14) to the one that is derived from the crack tip displacement field Equation E-9, one can determine the conic section coefficient

$$\bar{m} = \pi \left(\frac{\eta_o H}{2K_I \sqrt{a}} \right)^2 - 2 \qquad \text{(E-15)}$$

Thus, following Orange and substituting the stress intensity factor K_I, with the nondimensional stress intensity factor Y defined by the relation

$$K_I = Y\sigma\sqrt{a}$$

The value of $\bar{m}$ becomes;

$$\bar{m} = \pi \left[\frac{\eta_o H}{2Y\sigma a} \right]^2 - 2 \qquad \text{(E-16)}$$

where

$$Y = \frac{K}{\sigma\sqrt{a}} \qquad \text{(E-17)}$$

REFERENCES

1. A. A. Griffith, "Transactions Royal Society of London," Vol. 221, 1920 (this article has been published in Trans., ASM, 61, 1968, p. 871).

2. H. F. Bueckner, A Novel Principle for the Computation of Stress Intensity Factors. ZAMM, 50, 1970, pp. 529-546.

3. J. R. Rice, Some Remarks on Elastic Crack Tip Stress Fields. Technical Report, NASA NGL 40-002-08015, June 1971.

4. H. F. Bueckner, "Weight Functions for the Notched Bar," Zeitscheift für Angewandte Mathematik und Mechanik, Vol. 51, 1971, pp. 97-109.

5. P. C. Paris, R. M. McMeeking, and H. Tada, The Weight Function Method for Determining Stress Intensity Factors. MRL E-92. Material Research Laboratories, Brown University, 1975.

6. A. F. Grandt Jr, "Stress Intensity Factors for Some Through-Cracked Fastner Holes," International Journal of Fractures, Vol. 11, No. 2, April 1975.

7. H. J. Petroski and J. D. Achenbuch, "Computation of the Weight Function from a Stress Intensity Factor," Engineering Fracture Mechanics, Vol. 10, No. 2, pp. 257-266.

8. R. Labbens and Heliot Jr., 8th National Symposium of Fracture Mechanics. August 26-28, Brown University.

9. W. N. Sharpe Jr., and A. F. Grandt Jr., A Laser Interferometric Technique for Crack Surface Displacement Measurement. Air Force Material Laboratories, AFML-TR-74-75, July 1974.

10. D. E. Macha, W. N. Sharpe Jr., and A. F. Grandt Jr., A Laser Interferometry Method for Experimental Stress Intensity Factor Calibration, Cracks and Fracture. ASTM STP 601, American Society for Testing and Materials, 1976, pp. 490-505.

11. T. W. Orange, Crack Shapes and Stress Intensity Factors for Edge-Cracked Specimens Stress Analysis and Growth of Cracks. Proceedings of the 1971 National Symposium on Fracture Mechanics, Part I, ASTM STP 513, American Society for Testing and Materials, 1972, pp. 71-78.

12. H. Tada, P. C. Paris, and G. R. Irwin, The Stress Analysis of Cracks Handbook. DEL Research Corporation.

13. D. P. Rooke and D. J. Cartwright, Stress Intensity Factors.

REFERENCES (CONCLUDED)

14. A. F. Grandt Jr., Lecture Notes MC 6.05 Linear Elastic Fracture Mechanic. School of Engineering, Air Force Institute of Technology, Wright-Patterson AFB, 1978.

15. R. W. Hertzberg, Deformation and Fracture Mechanics of Engineering Materials. New York: John Wiley & Sons, Inc., 1976.

16. Damage Tolerant Design Handbook. MCIC-HB-01. Metals & Ceramics Information Center, Battelle-Columbus Laboratories, 1972.

17. J. Eftis, N. Subramonian, and H. Liebowitz, "Crack Border Stress and Displacement Equations Revisited, Engineering Fracture Mechanics, Vol. 9, 1977, pp. 189-210.

18. P. F. Packman, The Role of Interferometry in Fracture Studies. Vanderbilt University, Nashville, TN.

19. W. N. Sharpe Jr., and A. F. Grandt Jr., A Preliminary Study of Fatigue Crack Retardation Using Laser Interferometry to Measure Crack Surface Displacement, Mechanics of Crack Growth. ASTM STP 590. American Society for Testing and Materials, 1976, pp. 302-320.

20. B. Gross, E. Roberts Jr., and J. E. Srawley, "Elastic Displacements for Various Edge-Cracked Plate Specimens," The International Journal of Fracture Mechanics, Vol. 4, No. 3, September 1968.

21. A. F. Grandt Jr., Two Dimensional Stress Intensity Factor Solutions for Radically Cracked Rings. AFML-TR-75-121, Air Force Material Laboratories, Wright-Patterson Air Force Base.

22. G. R. Irwin, Fracturing of Metals. ASM, Cleveland, Ohio, 1949, p. 147.

23. J. P. Gallagher, What the Designer Should Know About Fracture Mechanics Fundamentals. Automotive Engineering Congress, Detroit, Michigan, January 1971.

24. R. W. Hornbeck, Numerical Methods, QPL Series. New York: Quantum Publishers, Inc.

25. Subprogram Library Guide. ASD Computer Center, Wright-Patterson Air Force Base, Ohio.

26. IMSL library Guide. IMSL, International Mathematical and Statistical Library, Houston, Texas.

27. S. P. Timoshenko and J. N. Goodier, Theory of Elasticity. New York: McGraw-Hill, 1969.

28. W. F. Brown Jr., and J. E. Srawley, Plane Strain Crack Toughness Testing of High Strength Metalic Materials. ASTM STP 410. American Society for Testing and Materials, 1967, p. 13.

ATE
MED
80